at 6 h (a 6.64-fold increase over sham), in IL-1α/β KO mice (Fig. 1B) compared with in WT after BCCAO. Also, the levels at 3 and 24 h in IL-6 KO mice (Fig. 1C) were significantly lower than in WT ($p < 0.01$, WT versus IL-6KO, respectively; data not shown).

IL-1β mRNA exhibited robust inductions for all time points in WT mice compared with the sham after BCCAO (Fig. 2A). The peak levels of IL-1β mRNA were approximately seven times higher than in sham observed at the 12-h time point and declined with time, but still showed a significant increase at least to 72 h. Additionally, as shown in Fig. 2B and C, the levels of IL-1β mRNA at all time points were lower in ischemic TNF-α KO mice and IL-6 KO mice than in WT.

IL-6 mRNA expression was markedly upregulated at all time points tested in ischemic mice compared to the sham. The first peak occurred at 6 h, followed by a second peak observed at 24 h in WT mice after BCCAO (Fig. 3A). Interestingly, as shown in Fig. 3B, the expression of IL-6 mRNA was markedly increased in ischemic TNF-α KO mice, with two induced peaks observed at 3 and 24 h, and the first peak earlier than that of the WT mice. After a slight decrease, IL-6 mRNA reached the second peak at 24 h in the TNF-α KO mice. While IL-6 mRNA levels remained elevated up to 72 h, the single peak observed at 12 h was notably later in IL-1α/β KO mice (Fig. 3C) compared with the first peak in WT after BCCAO. Indeed, there were statistically significant pattern differences in IL-6 among WT, TNF-α KO, and IL-1α/β KO mice ($p < 0.05$; data not shown).

This study investigated mRNA levels of pro-inflammatory cytokines and their interactions in the mouse hippocampus after cerebral ischemia. Following ischemic reperfusion, levels increased and demonstrated two peaks at 3 and 24 h for TNF-α, one peak at 12 h for IL-1β, and two peaks at 6 and 24 h for IL-6 in the WT mouse hippocampus, which are compatible with our data on cytokines in gerbils at the protein level [17]. All pro-inflammatory cytokine mRNA expressions tested in this study returned to near sham levels 72 h (pyramidal cell degeneration might have occurred in both WT and KO ischemic mice) following ischemia [8,12].

The responsive increase in TNF-α mRNA was lower in ischemic IL-6 KO mice than in WT mice, suggesting that the rapid expression of TNF-α mRNA is modulated by IL-6 in the early stage of ischemic reperfusion. At the same time, very low levels of IL-1β mRNA were demonstrated in ischemic TNF-α KO and IL-6 KO mice. Thus, these findings also indicate that TNF-α and IL-6 may enhance the rapid expressions of IL-1β mRNA via positive feedback mechanisms after transient cerebral ischemia. In addition, TNF-α and IL-1β could act as autocrine stimulators of astrocyte IL-6 production [18] and induce IL-6 gene expression directly in astrocytes, and exhibit a synergistic effect [4,16]. Therefore, the delayed peak of IL-6 mRNA in IL-1α/β KO mice compared with WT mice may suggest that expression of IL-6 mRNA was induced by IL-1β and/or TNF-α in the ischemic brain. Our present study also demonstrates a rapid and robust increase in IL-6 mRNA in ischemic TNF-α KO mice compared with in WT, which indicates a compensatory increase for a sustained lower level of IL-1β and TNF-α deficiency.

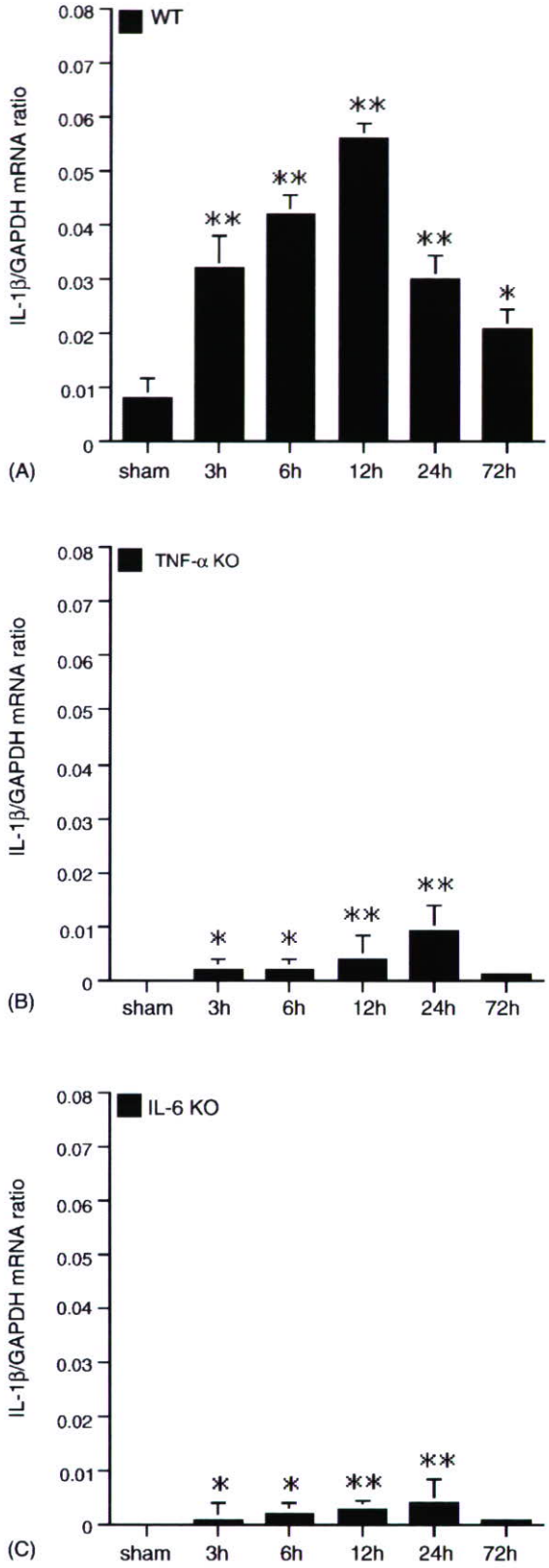

Fig. 2. Time courses of IL-1β mRNA expression in WT mice (A), TNF-α KO mice (B) and IL-6 KO (C) mice were determined using real-time PCR. Each data point represents the mean ± S.E.M. (sham = 2–3, ischemia = 5–6). $^{*}p < 0.05$, $^{**}p < 0.01$, compared with sham as determined by ANOVA. Note that brain mRNA levels in sham group are statistically different between WT and KO mice.

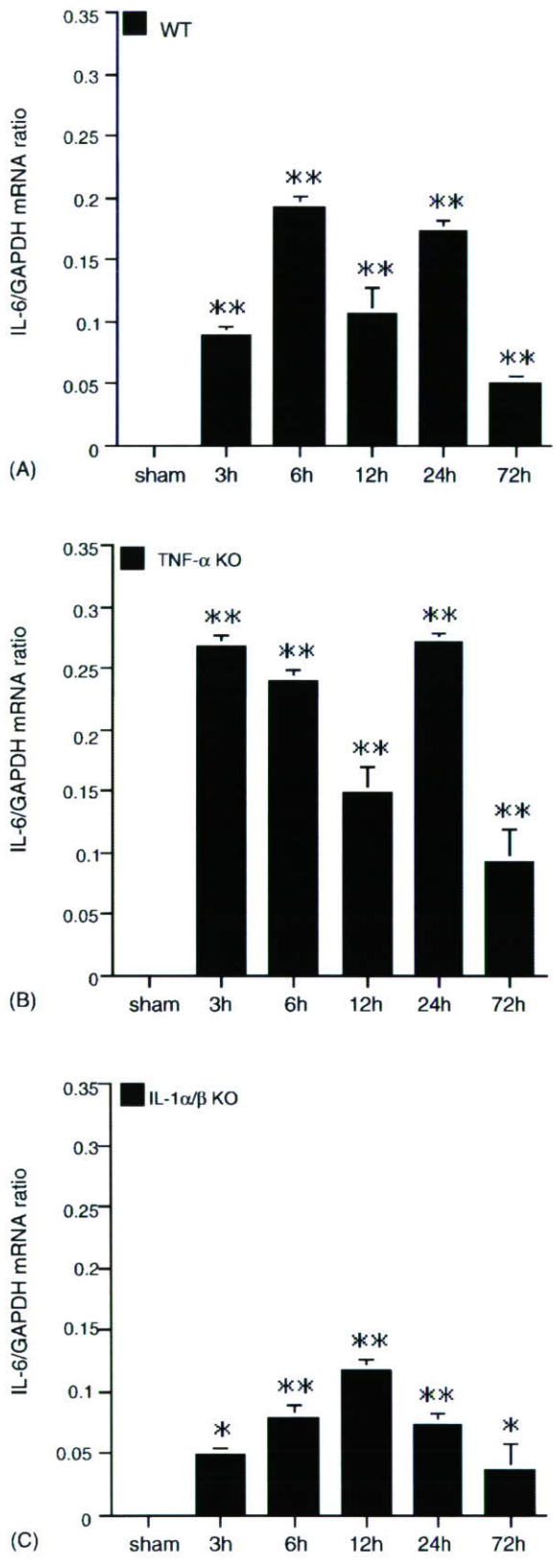

Fig. 3. Time courses of IL-6 mRNA expression in WT mice (A), TNF-α KO mice (B) and IL-1α/β KO mice (C) were determined using real-time PCR. Each data point represents the mean ± S.E.M. (sham = 2–3, ischemia = 5–6). $^{*}p < 0.05$, $^{**}p < 0.01$, compared with sham as determined by ANOVA.

Pro-inflammatory cytokines interact in the central nervous system, especially in microglia and astrocytes [3]. Although we have not examined the activation of glial cells in this study, there are convincing data that the brain resident cells such as microglia are rapidly activated following transient cerebral ischemia [9,14]. Further, the activated microglia are known to be the major source of TNF-α, IL-1β and IL-6 in acute brain ischemia [6,10,13]. Our most recent study demonstrated that the first early TNF-α mRNA expression peak derives from endogenous brain cells, and the secondary expression peak derives mainly from endogenous brain cells, but also from a few bone marrow-derived cells [15]. Thus, the increased pro-inflammatory cytokine levels observed at the early stage (<24 h) in transient global ischemia mainly originate from activated glial cells.

Since pro-inflammatory cytokine expression following cerebral ischemia is complex, further studies are necessary to confirm whether the different releasing patterns of the studied cytokines are dependent on still other cytokines following cerebral ischemia.

In summary, the present study demonstrates that the mRNA expressions of the three pro-inflammatory cytokines TNF-α, IL-1β and IL-6 in mice hippocampus exhibit different temporal patterns at the early stage of transient global ischemic reperfusion. The results from the various cytokine-KO mice indicate that one cytokine triggers the synthesis or release of several other cytokines in brain lesions following cerebral ischemia.

Acknowledgments

We are thankful to Yiwen Li (Foreign Researcher of the Japan Society for the Promotion of Science) for technical advice and helpful discussion, Dr A. Hara and Dr M. Takemura for expert technical assistance, and Mr. John Cole for proofreading the English of this manuscript.

References

[1] S.M. Allan, N.J. Rothwell, Cytokines and acute neurodegeneration, Nat. Rev. Neurosci. 2 (2001) 734–744.
[2] F.C. Barone, G.Z. Feuerstein, Inflammatory mediators and stroke: new opportunities for novel therapeutics, J. Cereb. Blood Flow Metab. 19 (1999) 819–834.
[3] E.N. Benveniste, Inflammatory cytokines within the central nervous system: sources, function, and mechanism of action, Am. J. Physiol. 263 (1992) C1–C16.
[4] E.N. Benveniste, S.M. Sparacio, J.G. Norris, H.E. Grenett, G.M. Fuller, Induction and regulation of interleukin-6 gene expression in rat astrocytes, J. Neuroimmunol. 30 (1990) 201–212.
[5] R. Berti, A.J. Williams, J.R. Moffett, S.L. Hale, L.C. Velarde, P.J. Elliott, C. Yao, J.R. Dave, F.C. Tortella, Quantitative real-time RT-PCR analysis of inflammatory gene expression associated with ischemia-reperfusion brain injury, J. Cereb. Blood Flow Metab. 22 (2002) 1068–1079.
[6] F. Block, M. Peters, M. Nolden-Koch, Expression of IL-6 in the ischemic penumbra, Neuroreport 11 (2000) 963–967.
[7] W.M. Clark, L.G. Rinker, N.S. Lessov, K. Hazel, J.K. Hill, M. Stenzel-Poore, F. Eckenstein, Lack of interleukin-6 expression is not protective against focal central nervous system ischemia, Stroke 31 (2000) 1715–1720.

[8] M. Fujii, H. Hara, W. Meng, J.P. Vonsattel, Z. Huang, M.A. Moskowitz, Strain-related differences in susceptibility to transient forebrain ischemia in SV-129 and C57black/6 mice, Stroke 28 (1997) 1805–1810 (discussion 1811).

[9] J. Gehrmann, P. Bonnekoh, T. Miyazawa, K.A. Hossmann, G.W. Kreutzberg, Immunocytochemical study of an early microglial activation in ischemia, J. Cereb. Blood Flow Metab. 12 (1992) 257–269.

[10] R. Gregersen, K. Lambertsen, B. Finsen, Microglia and macrophages are the major source of tumor necrosis factor in permanent middle cerebral artery occlusion in mice, J. Cereb. Blood Flow Metab. 20 (2000) 53–65.

[11] R. Horai, M. Asano, K. Sudo, H. Kanuka, M. Suzuki, M. Nishihara, M. Takahashi, Y. Iwakura, Production of mice deficient in genes for interleukin (IL)-1alpha, IL-1beta, IL-1alpha/beta, and IL-1 receptor antagonist shows that IL-1beta is crucial in turpentine-induced fever development and glucocorticoid secretion, J. Exp. Med. 187 (1998) 1463–1475.

[12] Y. Imaizumi, H. Mizushima, H. Matsumoto, K. Dohi, K. Matsumoto, H. Ohtaki, H. Funahashi, S. Matsunaga, R. Horai, M. Asano, Y. Iwakura, S. Shioda, Increased expression of interleukin-1beta in mouse hippocampus after global cerebral ischemia, Acta Histochem. Cytochem. 34 (2001) 357–362.

[13] T. Mabuchi, K. Kitagawa, T. Ohtsuki, K. Kuwabara, Y. Yagita, T. Yanagihara, M. Hori, M. Matsumoto, Contribution of microglia/macrophages to expansion of infarction and response of oligodendrocytes after focal cerebral ischemia in rats, Stroke 31 (2000) 1735–1743.

[14] T. Morioka, A.N. Kalehua, W.J. Streit, Progressive expression of immunomolecules on microglial cells in rat dorsal hippocampus following transient forebrain ischemia, Acta Neuropathol. (Berl.) 83 (1992) 149–157.

[15] Y. Murakami, K. Saito, A. Hara, Y. Zhu, K. Sudo, M. Niwa, H. Fujii, H. Wada, H. Ishiguro, H. Mori, M. Seishima, Increases in tumor necrosis factor-alpha following transient global cerebral ischemia do not contribute to neuron death in mouse hippocampus, J. Neurochem. 93 (2005) 1616–1622.

[16] J.G. Norris, E.N. Benveniste, Interleukin-6 production by astrocytes: induction by the neurotransmitter norepinephrine, J. Neuroimmunol. 45 (1993) 137–145.

[17] K. Saito, K. Suyama, K. Nishida, Y. Sei, A.S. Basile, Early increases in TNF-alpha, IL-6 and IL-1 beta levels following transient cerebral ischemia in gerbil brain, Neurosci. Lett. 206 (1996) 149–152.

[18] S.M. Sparacio, Y. Zhang, J. Vilcek, E.N. Benveniste, Cytokine regulation of interleukin-6 gene expression in astrocytes involves activation of an NF-kappa B-like nuclear protein, J. Neuroimmunol. 39 (1992) 231–242.

[19] T. Taniguchi, M. Takata, A. Ikeda, E. Momotani, K. Sekikawa, Failure of germinal center formation and impairment of response to endotoxin in tumor necrosis factor alpha-deficient mice, Lab. Invest. 77 (1997) 647–658.

[20] B. Viviani, S. Bartesaghi, E. Corsini, C.L. Galli, M. Marinovich, Cytokines role in neurodegenerative events, Toxicol. Lett. 149 (2004) 85–89.

[21] C.X. Wang, A. Shuaib, Involvement of inflammatory cytokines in central nervous system injury, Prog. Neurobiol. 67 (2002) 161–172.

[22] G. Yang, K. Kitagawa, K. Matsushita, T. Mabuchi, Y. Yagita, T. Yanagihara, M. Matsumoto, C57BL/6 strain is most susceptible to cerebral ischemia following bilateral common carotid occlusion among seven mouse strains: selective neuronal death in the murine transient forebrain ischemia, Brain Res. 752 (1997) 209–218.

[23] J. Zaremba, J. Losy, Cytokines in clinical and experimental ischemic stroke, Neurol. Neurochir. Pol. 38 (2004) S57–S62.

Available online at www.sciencedirect.com
SCIENCE DIRECT
Behavioural Brain Research 167 (2006) 355–364
BEHAVIOURAL BRAIN RESEARCH
www.elsevier.com/locate/bbr

Research report

Interleukin-1αβ gene-deficient mice show reduced nociceptive sensitivity in models of inflammatory and neuropathic pain but not post-operative pain

Prisca Honore [a,*], Carrie L. Wade [a], Chengmin Zhong [a], Richard R. Harris [a], C. Wu [b], Tariq Ghayur [b], Yoichiro Iwakura [c], Michael W. Decker [a], Connie Faltynek [a], James Sullivan [a], Michael F. Jarvis [a]

[a] *Abbott laboratories, Dept R4N5, Bldg AP9A-LL, 100 Abbott Park Road, Abbott Park, IL 60064, USA*
[b] *Abbott Bioresearch Center, Worcester, MA, USA*
[c] *Laboratory Animal Research Center, Institute of Medical Science, University of Tokyo, Japan*

Received 13 August 2005; received in revised form 27 September 2005; accepted 29 September 2005
Available online 26 October 2005

Abstract

The pro-inflammatory cytokine interleukin-1 (IL-1) has been implicated in both inflammatory processes and nociceptive neurotransmission. To further investigate the role of IL-1 in different pain states, gene-disrupted mice lacking both IL-1α and IL-1β genes (IL-1αβ (−/−)) were characterized in inflammatory, neuropathic, and post-operative pain models. IL-1αβ (−/−) mice showed normal sensorimotor function as measured by the rotorod assay compared to control mice (BALB/c). Acute and persistent formalin-induced nocifensive behaviors were reduced by 20% in IL-1αβ (−/−) mice as compared to control mice. IL-1αβ (−/−) mice also showed reduced inflammatory thermal and mechanical hyperalgesia compared to controls following the intraplantar administration of carrageenan or complete Freund's adjuvant (CFA). The duration of inflammatory hyperalgesia was shortened in IL-1αβ (−/−) mice versus controls in the CFA model. In contrast, deletion of IL-1αβ did not change the extent or the duration of post-operative pain developing after skin incision of the hind paw. Finally, time to onset, duration, and magnitude of mechanical allodynia were reduced in two models of neuropathic pain, spinal nerve L5–L6 ligation and chronic constriction injury of the sciatic nerve, in IL-1αβ (−/−) mice versus controls. These results demonstrate that IL-1αβ modulates both the generation and the maintenance of inflammatory and chronic neuropathic pain and that IL-1 may modulate nociceptive sensitivity to a greater extent in conditions of chronic as compared to acute pain.

Keywords: Cytokines; Chronic pain; Mirror-image pain

1. Introduction

Interleukin-1 (IL-1) is a major pro-inflammatory cytokine that has diverse actions in the CNS including modulation of nociceptive signaling [29]. Endogenous IL-1 levels are increased in the CNS in response to trauma or inflammation associated with mechanical damage, ischemia, seizures, and hyperexcitability [27]. Increased IL-1 concentrations in the CNS also result in dose-dependent modulation of nociceptive signaling with low doses producing hyperalgesia and high doses producing analgesia [2,13]. At the level of the spinal cord, blockade of IL-1 receptors with the IL-1 receptor antagonist (IL-1ra), generally results in reduced nociception in animal models of inflammation and nerve-injury-induced pain [16,22,24]. These findings are further supported by the demonstration that exogenously applied IL-1 produces hyperalgesia when applied peripherally [8].

The actions of IL-1 are mediated by two isoforms, IL-1α and IL-1β (see review in [7]). Both IL-1 isoforms bind to two distinct IL-1 receptors termed types I and II. The type I receptor requires a specific IL-1 receptor accessory protein (IL-1*acp*) for high affinity binding and signal transduction. The pro-inflammatory actions of both IL-1α and IL-1β are attributable to their interactions with the type I receptor. The type II receptor has no known biological function and may serve as a sink or decoy receptor.

* Corresponding author. Tel.: +1 847 938 0518; fax: +1 847 938 0072.
E-mail address: marie.honore@abbott.com (P. Honore).

0166-4328/$ – see front matter © 2005 Elsevier B.V. All rights reserved.
doi:10.1016/j.bbr.2005.09.024

In addition to the analgesic effects of the IL-1ra in experimental pain models, several genetic approaches have been used to further investigate the pronociceptive actions of IL-1 in mice. These include targeted gene disruption of the IL-1 Type I receptor or the IL-1*acp*, as well as, transgenic over-expression of the IL-1ra [31]. All of these approaches have produced mice that show reduced nociceptive responses to acute noxious thermal and mechanical stimulation relative to wild-type animals [31]. Despite the consistency of these results, little is known regarding the degree of cytokine compensation that may occur in these genetically disrupted animals. The putative mechanism by which IL-1 alters nociceptive neurotransmission also remains to be elucidated.

The targeted deletions of IL-1α, IL-1β, and the combined deletion of IL-1αβ in viable mice have been accomplished [12]. These mice are overtly indistinguishable from wild-type mice and reproduce normally. The inflammatory and immunological phenotypes of the mice have been extensively characterized and IL-1αβ (−/−) mice show the expected insensitivity to the pro-inflammatory effects of IL-1 [12,19].

To further understand the role of IL-1 in neuronal hyperexcitability and neurodegeneration, IL-1 gene disrupted mice have been studied for their susceptibility to transient brain ischemia [3]. Interestingly, mice lacking either IL-1α or IL-1β alone did not differ in their susceptibility to ischemia-induced brain damage, but IL-1αβ double-knockout mice were significantly protected as compared to wild-type controls [3]. Ischemic brain damage was also reduced by the IL-1ra in wild-type mice, but IL-1ra (−/−) mice show the same degree of infarct as wild-type mice [27]. Taken together, these data illustrate the potential compensatory regulation of IL-1 isoforms in IL-1α or IL-1β single-knockout animals. Because of these potential confounds, IL-1αβ double-knockout animals were used in this study to investigate the role of IL-1 in the development and maintenance of various pain states. While a variety of IL-1 signaling manipulations have been examined for effects on nociceptive sensitivity, and mice lacking IL-1αβ have been characterized for inflammatory and immune responses, the nociceptive sensitivity of IL-1αβ (−/−) has not been characterized. Thus, the aim of the present study was to further characterize the role of IL-1 in chronic pain states by examining mice lacking both forms of IL-1 (IL-1αβ) in a variety of inflammatory, neuropathic, and post-operative pain models.

2. Materials and methods

2.1. Animals

Homozygous BALB/c mice lacking IL-1αβ were backcrossed to BALB/c mice for at least eight generations as previously described [12,13]. Age-matched BALB/c mice were used as controls. Experiments were performed on adult male mice weighing 20–25 g. Mice were kept in a vivarium, maintained at 22 °C, with a 12 h alternating light–dark cycle with food and water available ad libitum. All experiments were performed during the light cycle. Animals were randomly divided into separate experimental groups. Each animal was used in one experiment only and was sacrificed immediately following the completion of the experiment. An Institutional Animal Care and Use Committee (IACUC) approved all animal handling and experimental protocols.

2.2. Zymosan-induced cytokine release

Zymosan-induced cytokine release was assessed as previously described [20,26]. Briefly, IL-1αβ (−/−) and BALB/c mice were injected intraperitonealy with 2 mg/animal zymosan (Sigma, St. Louis, MO) suspended in 0.9% saline. Four hours later the animals were euthanized by CO_2 inhalation and the peritoneal cavities lavaged 2× 1.5 ml with ice cold phosphate buffered saline (w/o Ca^{2+} and Mg^{2+}) with 10 units heparin/ml. For cytokine determination the samples were spun at 10,000 × *g* in a refrigerated microfuge (4 °C), supernatants removed and frozen until assayed. IL-1β and TNF-α levels were determination by ELISA (Endogen Rockford, IL). ELISAs were conducted according to manufacturer's instructions.

2.3. Formalin test

Following a 30 min acclimation period to individual observation cages, 25 μl of a 5% formalin solution was injected (s.c.) into the dorsal aspect of the right hind paw and the animals were then returned to the clear observation cages. Animals were observed for periods of time corresponding to phase 1 (0–10 min) and phase 2 (15–45 min) of the formalin test. Nociceptive behaviors were recorded from animals during the session by observing each animal for one 60 s observation period during each 5 min interval. Nociceptive behaviors recorded included flinching, licking or biting the injected paw.

2.4. Carrageenan- and complete Freund's adjuvant-induced inflammatory pain

Unilateral inflammation was induced by injecting 25 μl of a 2% solution of λ-carrageenan or 25 μl of a 50% solution of complete Freund's adjuvant (CFA) (Sigma Chemical Co., St. Louis, MO) in physiological saline into the plantar surface of the mouse right hind paw. In the carrageenan model, animals were tested for thermal hyperalgesia starting at 3 h after injection and then every day for 3 days and every other day up to day 17 after injection, time point for which control mice had returned to baseline values. For the CFA model, mice were tested for thermal hyperalgesia and mechanical allodynia at 3 h after injection and then every day for 7 days, time point for which control mice had returned to baseline values.

2.5. Spinal nerve (L5/L6) ligation

As previously described in detail by Kim and Chung [14] and adapted to mice, incision was made dorsal to the lumbo-sacral plexus. The paraspinal muscles (left side) were separated from the spinous processes, the L5 and L6 spinal nerves isolated, and tightly ligated with 3-0 silk suture. Following hemostasis, the wound was sutured and coated with antibiotic ointment. Sham animals underwent all surgical procedures but nerve ligation. The animals were allowed to recover and then placed in a cage with soft bedding for 5 days before behavioral testing for mechanical allodynia. Mice were tested every 3 days up to day 43 after surgery, time point at which there was no difference between sham and nerve injured animals in the control group.

2.6. Chronic constriction injury of the sciatic nerve

As previously described in detail by Bennett and Xie [1] and adapted to mice, an incision was made below the pelvis and the biceps femoris and the gluteous superficialis (right side) were separated. The sciatic nerve was exposed, isolated, and three loose ligatures (5-0 chromic catgut) were placed around it. Following hemostasis, the wound was sutured and coated with antibiotic ointment. Sham animals underwent all surgical procedures but nerve ligation. The animals were allowed to recover and then placed in a cage with soft bedding for 3 days before behavioral testing for mechanical allodynia. Mice were tested up to day 121 after surgery.

2.7. Skin incision-induced pain

As previously described by Brennan et al. [4] and adapted to mice [21], a 0.5 cm longitudinal incision was made through the skin and fascia of the

plantar aspect of the foot, starting 0.2 cm from the proximal edge of the heel and extending toward the toes. The plantaris muscle was elevated and incised longitudinally with origin and insertion of the muscle remaining intact. The skin was then closed with 1 mattress suture (8-0 nylon). After surgery, the animals were allowed to recover and housed individually with soft bedding. Animals were tested for mechanical allodynia using von Frey hairs for 6 days after surgery.

2.8. Mechanical allodynia

Mechanical (tactile) allodynia was measured using calibrated von Frey filaments (Stoelting, Wood Dale, IL). Briefly, animals were placed into individual Plexiglas containers and allowed to acclimate for 30 min before testing. Withdrawal threshold was determined by increasing and decreasing stimulus intensity and estimated using a Dixon non-parametric test [5].

2.9. Thermal hyperalgesia

Thermal hyperalgesia was determined using a commercially available thermal paw stimulator described by Hargreaves et al. [11]. Animals were placed into individual plastic cubicles mounted on a glass surface maintained at 30 °C, and allowed a 20 min habituation period. A thermal stimulus, in the form of radiant heat emitted from a focused projection bulb, was then applied to the plantar surface of each hind paw. The stimulus current was maintained at 4.50 ± 0.05 A, and the maximum time of exposure was set at 20.48 s to limit possible tissue damage. The elapsed time until a brisk withdrawal of the hind paw from the thermal stimulus was recorded automatically using photodiode motion sensors. The right and left hind paw of each animal was tested in three sequential trials at approximately 5 min intervals. Paw withdrawal latency (PWL) was calculated as the mean of the two shortest latencies.

2.10. Motor performance

Rotorod performance was measured using an accelerating rotorod apparatus (Omnitech Electronics, Inc., Columbus, OH) as previously described [15]. For the rotorod assay, animals were allowed a 30 min acclimation period in the testing room and then placed on a rod that increased in speed from 0 to 20 rpm over a 60 s period. The time required for the animal to fall from the rod was recorded, with a maximum score of 60 s. Each animal was given three training sessions.

2.11. Statistics

Analysis of the in vivo data was carried out using analysis of variance (ANOVA, repeated measure for time-course in the carrageenan, CFA, Chung, Bennett, and skin incision models). Where appropriate, Fisher's protected least significant difference (FPLSD) was used for post hoc analysis. The level of significance was set at $p < 0.05$. Data are presented as mean ± S.E.M.

3. Results

3.1. General behavior

IL-1αβ (−/−) mice were not significantly different from BALB/c controls in overt behavior or in motor performance as assessed by rotorod performance ($p > 0.05$). The latency of BALB/c mice to fall in the rotorod test was 64.7 ± 3.8 s. The latency to fall for IL-1αβ (−/−) mice was 60.0 ± 3.9 s.

3.2. Inflammation-induced cytokine accumulation

Intraperitoneal administration of zymosan to BALB/c mice produced a significant accumulation of IL-1β and TNFα as measured by peritoneal gavage 4 h post-zymosan administration (Fig. 1). In contrast, similar zymosan treatment of IL-1αβ (−/−) mice resulted in no detectable accumulation of IL-1β, but a significant increase in TNFα levels in the peritoneal cavity. The magnitude of the zymosan-induced TNFα accumulation in IL-1αβ (−/−) mice was not significantly different than that of BALB/c mice (Fig. 1).

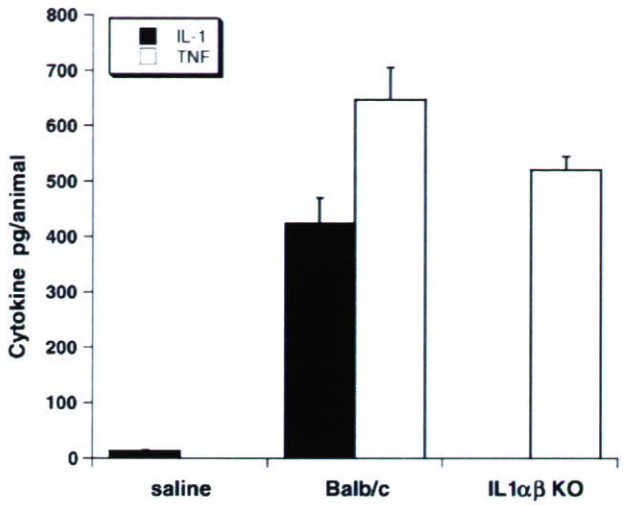

Fig. 1. Mouse peritoneal cytokine accumulation 4 h following intraperitoneal zymosan injection (2 mg/mouse).

3.3. Formalin-induced nociception

Following the intradermal administration of 5% formalin, IL-1αβ (−/−) mice showed a small (20–25%), but statistically significant ($p < 0.05$) reduction in nociceptive paw flinching compared to wild-type BALB/c mice (Fig. 2). The magnitude of this difference was similar in both the acute (0–10 min) and persistent (10–45 min) phases of the formalin response.

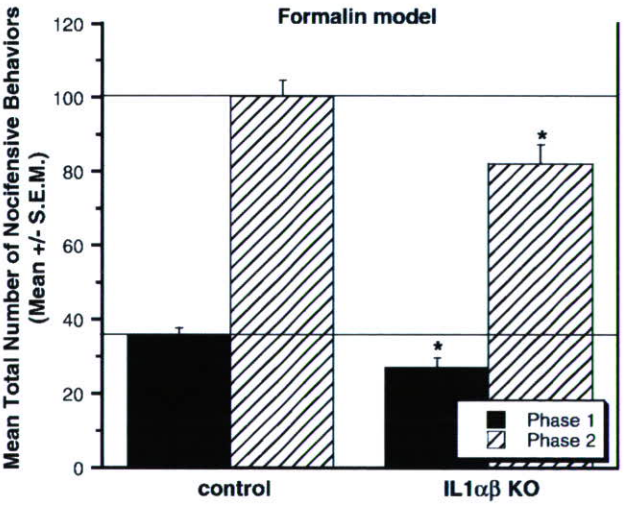

Fig. 2. IL-1αβ (−/−) mice show a decrease in spontaneous pain observed in both the first ($F(1, 44) = 7.02, p < 0.02$) and second phase ($F(1, 44) = 7.20, p < 0.02$) of the formalin response. Data represent mean ± S.E.M. $^{*}p < 0.05$ IL-1αβ (−/−) vs. control animals ($n = 23$ per experimental group).

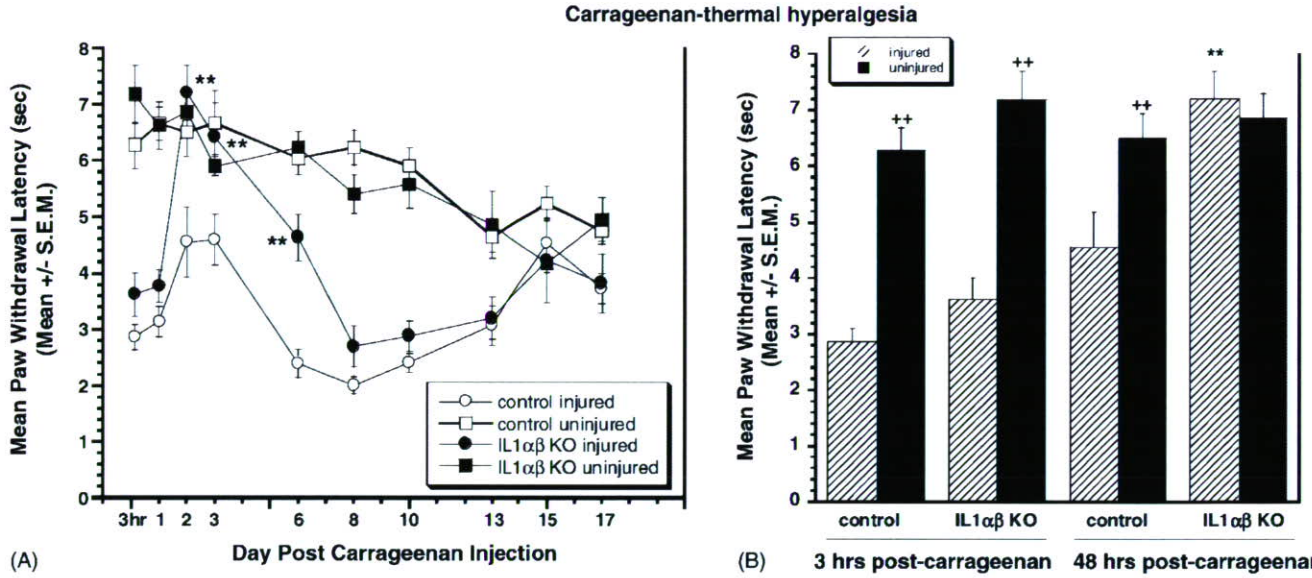

Fig. 3. IL-1αβ (−/−) mice show a decrease in carrageenan-induced thermal hyperalgesia (A). Repeated ANOVA showed a significant decrease in paw withdrawal latency between injured and uninjured paws in control mice ($F(1, 16) = 76.72$, $p < 0.0001$) and IL-1αβ (−/−) mice ($F(1, 14) = 25.29$, $p < 0.001$). Repeated ANOVA also demonstrated a significant difference between paw withdrawal latency on the injured paw between control and IL-1αβ (−/−) mice ($F(1, 15) = 6.40$, $p < 0.02$), but not on the uninjured paw ($F(1, 15) = 3.402$, $p = 0.08$). Data represent mean ± S.E.M. $^{*}p < 0.05$, $^{**}p < 0.01$ IL1 KO vs. control animals ($n = 12$ per experimental group). (B) shows data at 3 and 48 h after carrageenan injection. Data represent mean ± S.E.M. $^{*}p < 0.05$, $^{**}p < 0.01$ IL-1αβ (−/−) vs. control animals. $^{++}p < 0.01$ injured vs. uninjured paw for each group.

3.4. Carrageenan-induced thermal hyperalgesia

The intraplantar administration of carrageenan produced a significant decrease in paw withdrawal latencies to a thermal heat source in both IL-1αβ (−/−) and BALB/c mice 3 h post-injection that persisted for 24 h (Fig. 3). At the 3 h time point there was no significant difference ($p > 0.05$) in the thermal hyperalgesic responses of IL-1αβ (−/−) and BALB/c mice. However, by 48 h, the IL-1αβ (−/−) mice had paw withdrawal latencies for the injured paw that were not significantly different from the uninjected paw or from uninjured BALB/c control mice (Fig. 3). At the 48 h time point, BALB/c control mice showed an attenuated hyperalgesic response, but had paw withdrawal latencies for the injured paw that were significantly different from the uninjured paw. This difference in thermal hyperalgesia sensitivity for the IL-1αβ (−/−) and BALB/c mice was maintained at day 3, but attenuated at day 6 post-carrageenan administration.

Interestingly, the carrageen-induced thermal hyperalgesic response for both the IL-1αβ (−/−) and BALB/c mice was biphasic such that by 8 days post-carrageenan administration both groups of mice has returned to a hyperalgesic state that persisted until 15 days post-carrageenan administration. While there appeared to be a decrease in paw withdrawal latencies for the uninjured (BALB/c and IL-1αβ (−/−) mice) from days 3 to 17, this trend was not statistically significant ($p > 0.05$).

3.5. CFA-induced thermal hyperalgesia and mechanical allodynia

Following the intraplantar administration of CFA, both IL-1αβ (−/−) and BALB/c mice developed significant thermal hyperalgesia and mechanical allodynia (Fig. 4). Both thermal hyperalgesia and mechanical allodynia were most prominent 3–48 h following CFA administration and the magnitude of this response in both IL-1αβ (−/−) and BALB/c mice returned to control (uninjured) levels by 5 days post-injection. The IL-1αβ (−/−) mice showed a statistically significant attenuated thermal hyperalgesic response and a faster recovery as compared to the BALB/c mice (Fig. 4A). A similar pattern of nociceptive responses for the IL-1αβ (−/−) mice was also observed for mechanical allodynia (Fig. 4B). However, IL-1αβ (−/−) mice showed less thermal hyperalgesia as compared to mechanical llodynia during the first 48 h following CFA treatment. Consistent with the recovery from thermal hyperalgesia, mechanical allodynia responses for IL-1αβ (−/−) returned to normal levels faster than for BALB/c mice (3 days versus 5 days following CFA injection).

3.6. Neuropathic pain

3.6.1. Spinal nerve ligation

Five days following spinal nerve ligation, tactile allodynia thresholds were not significantly different between injured and sham control paws for both the IL-1αβ (−/−) and BALB/c mice (Fig. 5). However, during the subsequent 6 days, tactile allodynia thresholds for the BALB/c mice markedly decreased to 0.1 + 0.0 gm on day 12. IL-1αβ (−/−) mice also developed significant tactile allodynia over this same time period compared to sham-operated controls. However, the magnitude of the mechanical response in IL-1αβ (−/−) mice was significantly attenuated relative to that observed for BALB/c mice. Fig. 5B shows the relative differences in tactile allodynia thresholds for both IL-1αβ (−/−) and BALB/c mice during the maximal allodynic period observed for the BALB/c mice (days 12–22).

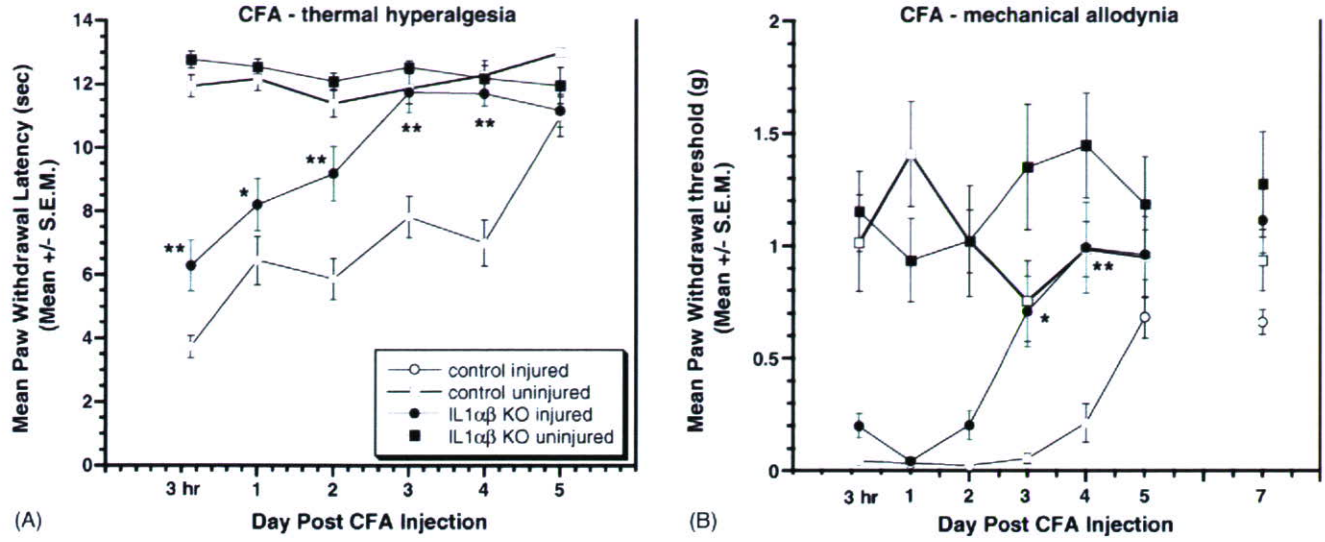

Fig. 4. IL-1αβ (−/−) mice show a decrease in CFA-induced thermal hyperalgesia (A) and mechanical allodynia (B). In (A), repeated ANOVA showed a significant decrease in paw withdrawal latency between injured and uninjured paws in control mice ($F(1, 22) = 252.74$, $p < 0.0001$) and IL-1αβ (−/−) mice ($F(1, 22) = 60.87$, $p < 0.0001$). Repeated ANOVA also demonstrated a significant difference between paw withdrawal latency of the injured paw between control and IL-1αβ (−/−) mice ($F(1, 22) = 43.03$, $p < 0.0001$), but not of the uninjured paw ($F(1, 22) = 1.34$, $p = 0.26$). In (B), repeated ANOVA showed a significant decrease in paw withdrawal threshold between injured and uninjured paws in control mice ($F(1, 15) = 42.13$, $p < 0.0001$) and IL1 KO mice ($F(1, 22) = 9.89$, $p < 0.01$). Repeated ANOVA also demonstrated a significant difference between paw withdrawal threshold of the injured paw between control and IL-1αβ (−/−) mice ($F(1, 22) = 21.42$, $p < 0.0001$), but not of the uninjured paw ($F(1, 15) = 0.84$, $p = 0.37$). Data represent mean ± S.E.M. $^{*}p < 0.05$, $^{**}p < 0.01$ IL-1αβ (−/−) vs. control animals ($n = 12$ per experimental group).

Throughout the 43-day testing period, no significant differences were found between the tactile allodynia responses of sham-operated IL-1αβ (−/−) and BALB/c mice. The differences in tactile allodynia responses for IL-1αβ (−/−) and BALB/c mice persisted for approximately 30 days following spinal nerve ligation. After which, tactile allodynia responses between IL-1αβ (−/−) and BALB/c mice were no longer significantly different (Fig. 5A).

In order to further characterize the nature of the nociceptive state of IL-1αβ (−/−) and BALB/c mice in the spinal nerve lig-

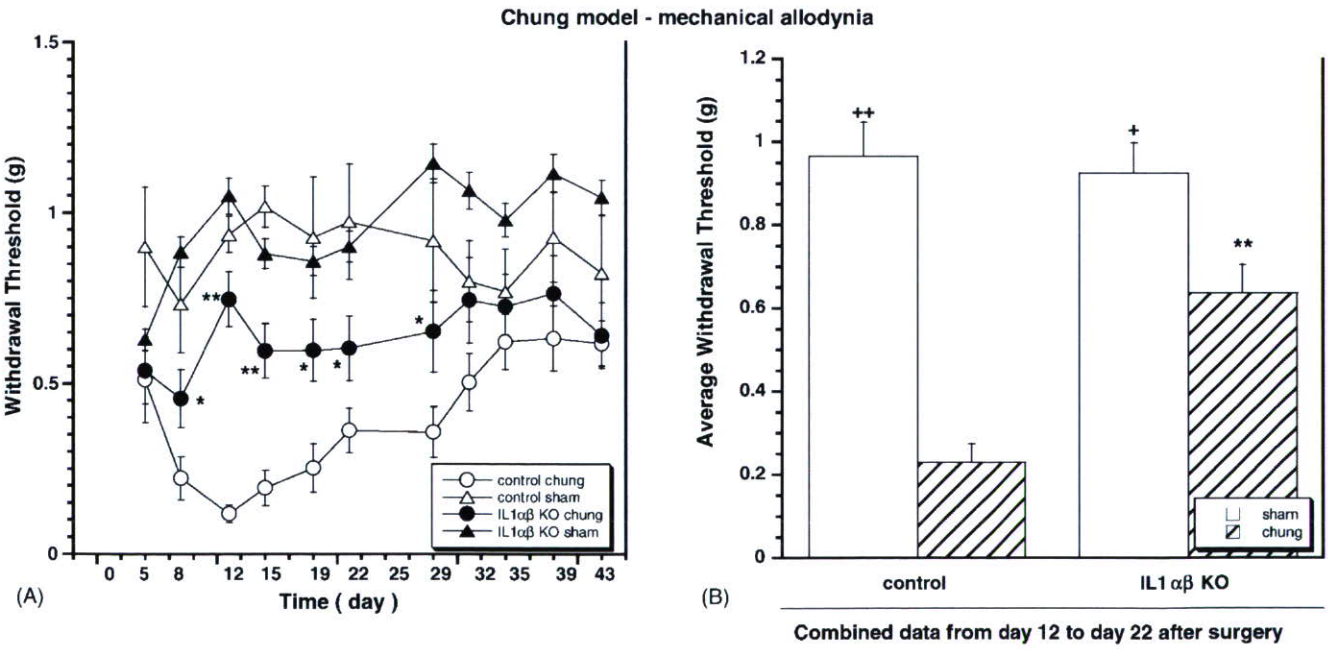

Fig. 5. IL-1αβ (−/−) mice show a decrease in mechanical allodynia observed after L5–L6 spinal nerve ligation (Chung model). Four groups of mice were evaluated in this study: sham surgery in controls ($n = 5$) and in IL-1αβ (−/−) mice ($n = 5$) and Chung surgery in control ($n = 14$) and IL1 KO mice ($n = 14$). Data represent mean ± S.E.M. $^{*}p < 0.05$, $^{**}p < 0.01$ IL-1αβ (−/−) vs. control animals. As seen on (A) when comparing the ipsilateral side to the injury in both sham and Chung animals in control and IL-1αβ (−/−) mice, it was shown that mechanical allodynia developed in control Chung animals vs. control shams (repeated ANOVA $F(1, 16) = 45.92$, $p < 0.0001$) and in IL-1αβ (−/−) Chung animals vs. IL-1αβ (−/−) shams (repeated ANOVA $F(1, 16) = 13.04$, $p < 0.01$). In addition, mechanical allodynia was significantly reduced in IL-1αβ (−/−) Chung mice vs. control Chung (repeated ANOVA $F(1, 25) = 17.51$, $p < 0.001$). However, there was no significant difference between mechanical threshold in sham control mice and sham IL-1αβ (−/−) mice (repeated ANOVA $F(1, 8) = 1.98$, $p = 0.20$). (B) Data grouped for days 12–22 after surgery. Data represent mean ± S.E.M. $^{*}p < 0.05$, $^{**}p < 0.01$ IL-1αβ (−/−) vs. control animals, $^{++}p < 0.01$ sham vs. Chung for each type of mice.

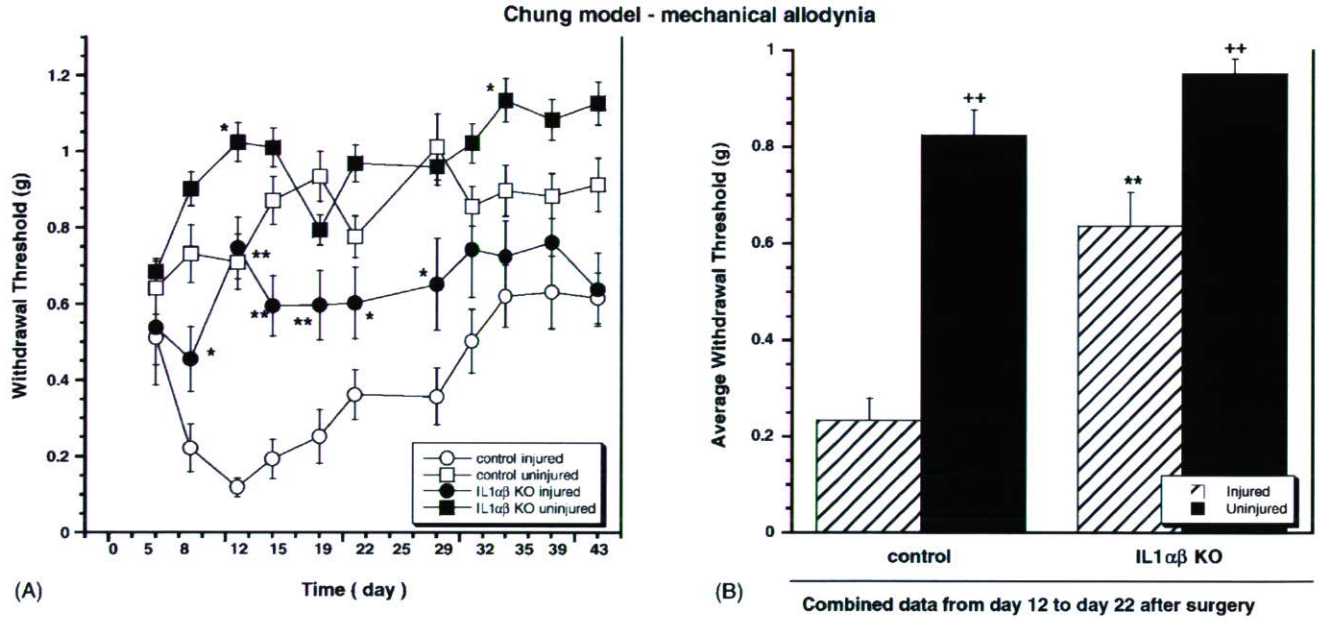

Fig. 6. IL-1αβ (−/−) mice show a decrease in mechanical allodynia observed after L5–L6 spinal nerve ligation (Chung model). Data represent mean ± S.E.M. $^{*}p < 0.05$, $^{**}p < 0.01$ IL-1αβ (−/−) vs. control animals. As seen on (A) Chung surgery-induced mechanical allodynia was more pronounced in control animals than in IL-1αβ (−/−) mice when comparing injured vs. uninjured paws (Repeated ANOVA for control mice, injured/uninjured paws $F(1, 26) = 113.08$, $p < 0.0001$; Repeated ANOVA for IL-1αβ (−/−) mice, injured/uninjured paws $F(1, 24) = 36.44$, $p < 0.0001$; Repeated ANOVA for the injured side between control and IL-1αβ (−/−) mice $F(1, 25) = 17.51$, $p < 0.001$). (B) shows data grouped from days 12 to 22 after surgery. Data represent mean ± S.E.M. $^{*}p < 0.05$, $^{**}p < 0.01$ IL-1αβ (−/−) vs. control animals, $^{++}p < 0.01$ injured vs. uninjured side for each group.

ation model, tactile allodynia threshold differences between the injured (ipsilateral) and uninjured (contralateral) paws of these mice were also examined (Fig. 6). Similar to the data shown in Fig. 5, significant tactile allodynia rapidly developed in the injured paws of BALB/c mice, while nociceptive responses in the injured paws of IL-1αβ (−/−) mice were significantly attenuated. In contrast to the data shown in Fig. 5, tactile allodynia thresholds for the uninjured paw of IL-1αβ (−/−) mice tended to be higher than those of BALB/c mice and were statistically significant on days 12 and 33.

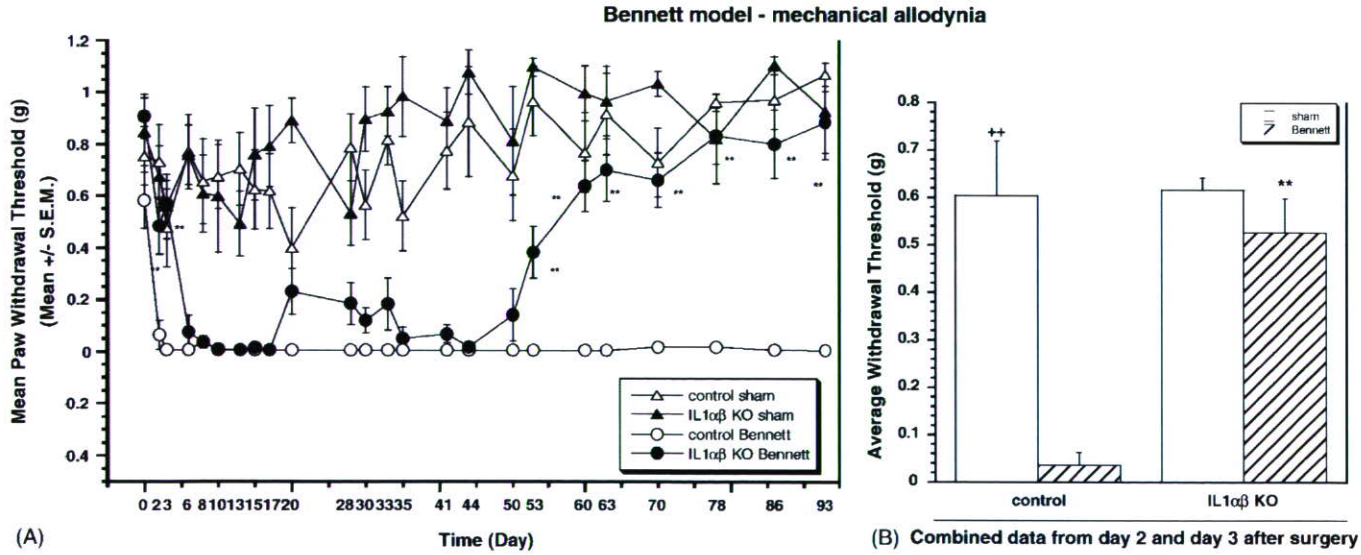

Fig. 7. IL-1αβ (−/−) mice show a decrease in mechanical allodynia observed after sciatic nerve injury (Bennett model). Four groups of mice were evaluated in this study: sham surgery in controls ($n = 6$) and in IL1 KO mice ($n = 6$) and Bennett surgery in control ($n = 14$) and IL-1αβ (−/−) mice ($n = 14$). Data represent mean ± S.E.M. $^{*}p < 0.05$, $^{**}p < 0.01$ IL1 KO vs. control animals. As seen on (A) when comparing the ipsilateral side to the injury in both sham and Bennett animals in control and IL-1αβ (−/−) mice, it was shown that while a strong mechanical allodynia developed in control Bennett animals vs. control shams (repeated ANOVA $F(1, 14) = 217.49$, $p < 0.0001$), mechanical allodynia developed in the IL-1αβ (−/−) mice (repeated ANOVA $F(1, 15) = 96.67$, $p < 0.0001$) in a slower manner and recovered faster so that at day 60 after surgery, the IL-1αβ (−/−) mice were fully recovered while the control Bennett mice were still fully allodynic (repeated ANOVA $F(1, 19) = 111.88$, $p < 0.0001$, between Bennett control mice and IL-1αβ (−/−) mice). There was no significant difference between the control shams and the IL-1αβ (−/−) shams (repeated ANOVA $F(1, 10) = 1.31$, $p = 0.28$). (B) Data grouped for days 2 and 3 after surgery. Data represent mean ± S.E.M. $^{*}p < 0.05$, $^{**}p < 0.01$ IL-1αβ (−/−) vs. control animals, $^{++}p < 0.01$ sham vs. Bennett for each type of mice.

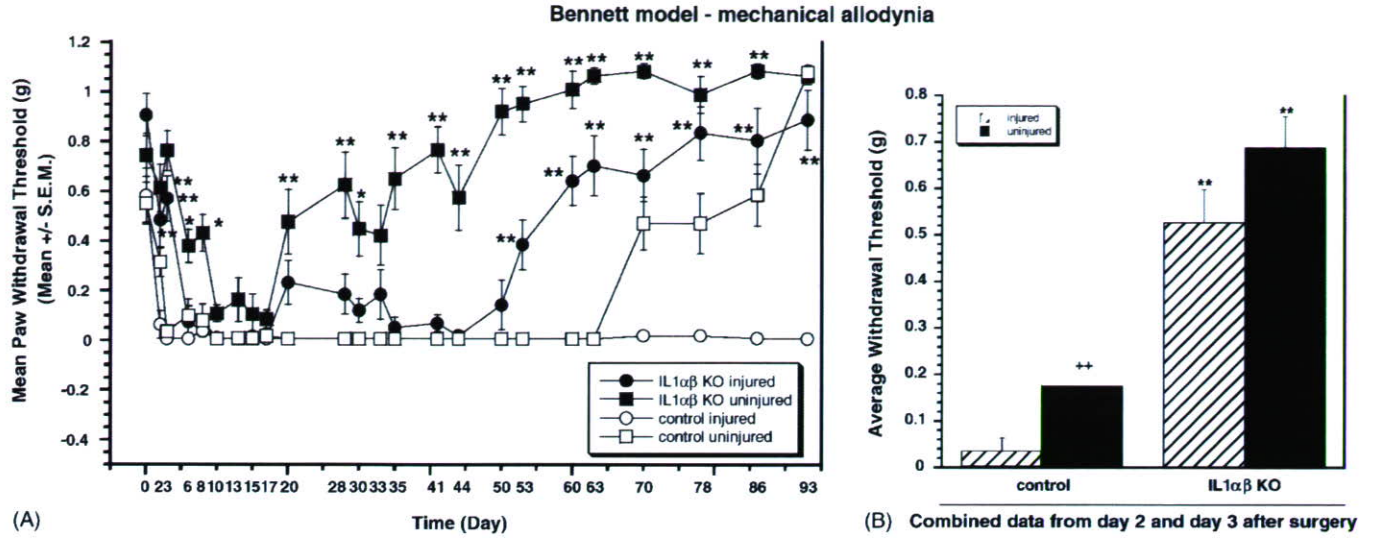

Fig. 8. IL-1αβ (−/−) mice show a decrease in mechanical allodynia observed after sciatic nerve injury (Bennett model). As seen in (A), Bennett surgery in both types of mice-induced mechanical allodynia on both the injured and uninjured side. However, mechanical allodynia was slower to develop and recovered faster in IL-1αβ (−/−) vs. control mice as shown by significant repeated ANOVA between control animals and IL-1αβ (−/−) animals for the injured side ($F(1, 19) = 111.88$, $p < 0.0001$) and uninjured side ($F(1, 19) = 344.00$, $p < 0.0001$). Data represent mean ± S.E.M. $^{*}p < 0.05$, $^{**}p < 0.01$ IL-1αβ (−/−) vs. control animals. (B) Data grouped from days 12 to 22 after surgery. Data represent mean ± S.E.M. $^{*}p < 0.05$, $^{**}p < 0.01$ IL-1αβ (−/−) vs. control animals, $^{++}p < 0.01$ injured vs. uninjured side for each group.

3.6.2. Chronic constriction injury of the sciatic nerve

Within 2–3 days following surgery, BALB/c control mice developed marked decreases in tactile allodynia thresholds as compared to sham-operated controls (Fig. 7). During this initial time following surgery, IL-1αβ (−/−) mice showed significantly less tactile allodynia (Fig. 7B). However, during the next 2 days, tactile allodynia thresholds for IL-1αβ (−/−) mice decreased to the same levels as the BALB/c mice. Both IL-1αβ (−/−) and Blab/c mice continues to show similar levels of tactile allodynia until approximately 50 days post-surgery after which the IL-1αβ (−/−) began to recover normal levels of tactile sensitivity. By 60 days post-surgery, the tactile allodynia thresholds of IL-1αβ (−/−) mice were not significantly different from sham-operated controls.

In order to further characterize the nature of the nociceptive state of IL-1αβ (−/−) and BALB/c mice in the CCI model, tactile allodynia threshold differences between the injured (ipsilateral) and uninjured (contralateral) paws of these mice were also examined (Fig. 8). Unlike the data shown in Fig. 7, significant tactile allodynia rapidly developed with a similar temporal pattern for both the injured (ipsilateral) and uninjured (contralateral) paws of BALB/c mice. The IL-1αβ (−/−) mice also developed tactile allodynia in both paws but the onset of nociception was delayed for the injured paw relative to the BALB/c mice. The development of tactile allodynia for the uninjured paw of IL-1αβ (−/−) mice was also delayed relative to that for the injured paw. The duration of tactile allodynia was more transient for the IL-1αβ (−/−) mice as compared to the BALB/c mice with the uninjured paw (contralateral) showing a significantly faster recovery to baseline tactile allodynia thresholds relative to the injured paws for both IL-1αβ (−/−) and BALB/c mice. There was no evidence of recovery of tactile allodynia thresholds for the injured paw of BALB/c mice by 90 days post-surgery.

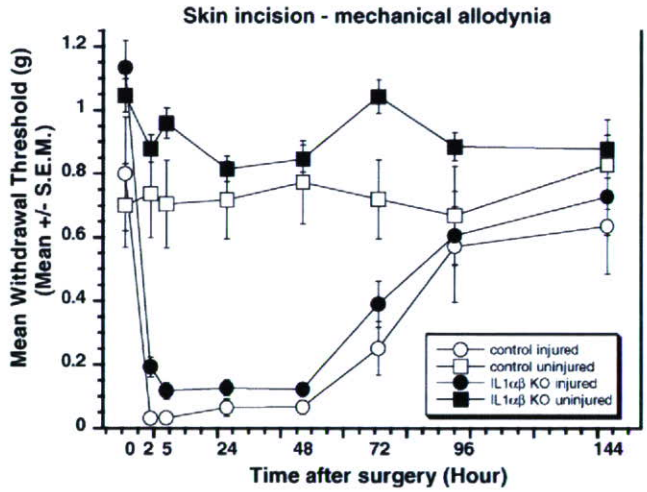

Fig. 9. IL-1αβ (−/−) mice developed as much post-operative pain as the control mice. Data represent mean ± S.E.M.

3.7. Skin incision-induced pain

Longitudinal incision through the skin and fascia of the plantar aspect of the foot results in the rapid development of tactile allodynia within 2 h post-surgery for both IL-1αβ (−/−) and BALB/c (Fig. 9). Allodynic responses persisted for approximately 3 days following the surgical injury and no significant differences between IL-1αβ (−/−) and BALB/c mice were noted. By 4 days post-surgery, tactile allodynia thresholds for both IL-1αβ (−/−) and BALB/c mice were not significantly different from those of their respective uninjured paws.

4. Discussion

The present data demonstrate that IL-1αβ (−/−) mice show reduced nociceptive sensitivity compared to control mice in

models of inflammatory and nerve injury-induced pain. However, both the magnitude and topography of the reduced nociceptive sensitivity exhibited by IL-1αβ (−/−) mice, as compared to BALB/c mice, were model-dependent. IL-1αβ (−/−) mice did not show any overt behavioral differences or altered motor performance compared to BALB/c controls. Additionally, the nociceptive sensitivity of the uninjured paws of IL-1αβ (−/−) mice to either mechanical or thermal stimulation did not differ from control animals. However, the ability of IL-1αβ (−/−) mice to produce IL-1 in response to an intraperitoneal zymosan challenge was completely suppressed. It has been previously reported that IL-1αβ (−/−) mice have normally developed thymus, spleen, and lymph nodes, as well as normal B and T cell function compared to control mice [18]. However, interactions between T cells and antigen-presenting cells are impaired [18] and IL-1αβ (−/−) mice show reduced LPS-stimulated increases in serum cortisol compared to wild-type mice [12]. Additionally, in IL-1αβ (−/−) mice intraperitoneally administered turpentine produces a diminished febrile response compared to control mice [12]. IL-1αβ (−/−) mice also show diminished COX-2, but not COX-1, expression in brain compared to control mice [12]. All of these effects are attributable to a specific disruption of IL-1β signaling in IL-1αβ (−/−) mice [12]. Consistent with previous results [12], the present data show that IL-1αβ (−/−) mice did not differ from BALB/c controls in their ability to generate zymosan-induced TNFα.

IL-1αβ (−/−) mice displayed a small, but statistically significant reduction in nociceptive sensitivity in the acute phase of the formalin test. This finding is in agreement with the reported effects of other genetically based IL-1 signaling perturbations on acute nociceptive responses [31]. Interestingly, a similar effect was observed in the persistent phase of the formalin test indicating that IL-1 may contribute to sensitization of the nervous system in response to ongoing nociceptive sensory input [10]. However, IL-1αβ (−/−) mice did not differ from controls in their sensitivity to skin incision-induced pain. This model of post-incisional pain is characterized by a highly specific pharmacology in which the excitatory amino acid AMPA may play a more prominent role in nociceptive signaling than other glutamatergic mechanisms [32] and the present data indicate that IL-1 involvement may be minimal.

In models of prolonged inflammatory pain, IL-1αβ (−/−) mice initially displayed transient, but robust, thermal and/or or mechanical hyperalgesia that resolved over time resulting in an overall attenuated pain response as compared to BALB/c control mice. The transient recovery of nociceptive thresholds for both control and IL-1αβ (−/−) mice in the carrageenan thermal hyperalgesia model is consistent with a previous report [23], however, IL-1αβ (−/−) mice showed a more significant recovery such that thermal hyperalgesia was completely eliminated. While IL-1αβ (−/−) CFA-mice developed as much mechanical allodynia as their BALB/c controls but recovered faster, the effects of IL-1αβ (−/−) on mechanical allodynia in 2 models of neuropathic pain were different. In a spinal nerve ligation model of neuropathic pain, IL-1αβ (−/−) mice showed a consistent pattern of reduced mechanical allodynia as compared to control mice. In a chronic constriction injury of the sciatic nerve model, BALB/c mice rapidly developed mechanical allodynia that remained stable for at least 90 days. However, IL-1αβ (−/−) mice were initially protected and developed allodynia more slowly that BALB/c mice. Interestingly, IL-1αβ (−/−) mice also completely recovered normal tactile allodynia thresholds by 60 days post-surgery, paralleling what was observed in the recovery phase of the CFA model of chronic inflammatory pain and clearly contrasting to the lack of changes in mechanical allodynia observed in the post-operative pain model. These contrasting results obtained with the same modality of pain in various models of acute and chronic inflammatory and neuropathic pain outline that IL-1αβ (−/−) plays a differential role in different types of pain and that even in the same category of pain such as neuropathic pain, IL-1αβ (−/−) can play different roles in the initiation and maintenance of mechanical allodynia depending on the model.

In both the spinal nerve ligation and chronic constriction injury models of neuropathic pain, the degree of tactile allodynia for the injured paw in IL-1αβ (−/−) and control mice was compared to both the uninjured contralateral paw as well as to sham-operated mice. For the spinal nerve ligation model, tactile allodynia thresholds were similar for uninjured contralateral paws of IL-1αβ (−/−) and control mice and for sham-operated controls. Thus, the degree of tactile allodynia found for the injured paws in this model of neuropathic pain was similar regardless of how control responses were assessed. In contrast, there were significant differences in tactile allodynia thresholds between sham-operated and uninjured contralateral paws in the chronic constriction injury model of neuropathic pain. Following nerve injury in this model, tactile allodynia thresholds for both the injured and uninjured paws were significantly reduced. Interestingly, nociceptive responses for the uninjured paws of IL-1αβ (−/−) mice recovered most quickly as compared of the injured paw of IL-1αβ (−/−) mice or injured and uninjured paws of control mice. These findings highlight differences in the expression of allodynia in these two models of neuropathic pain and highlight the necessity for including comparisons to sham-operated animals. In addition, these results demonstrate the development of mirror-image pain following chronic constriction injury of the sciatic nerve in mice. Furthermore, the results obtained in the IL-1αβ (−/−) mice suggest that IL-1 plays a role in the generation and maintenance of mirror-image pain at least in the chronic constriction injury model of neuropathic pain. Mirror-image pain is an enigmatic phenomenon with unknown etiology that has been reported during the course of multiple clinical pain syndromes and is predominantly associated with trauma or inflammation to peripheral nerves (see Ref. [28]). While neuropathic pain can be accounted for, in part, by ectopic action potential firing and hyperexcitability in the injured nerve, no abnormal activity has been reported in the healthy contralateral nerve. Thus, events initiated at the site of injury most likely lead to mirror-image pain changes via central sensitization. Mirror-image pain has been previously described in a model of sciatic inflammatory neuropathy (SIN) in rats induced by peri-neural zymosan injection [17,28]. Interestingly, in this model, while low levels of immune activation create a unilateral mechanical allodynia ipsilateral to the inflamed sciatic nerve, stronger

immune activation creates both ipsilateral allodynia and mirror-image pain. In two recent studies, it was shown that induction of ipsilateral and mirror-image allodynias were blocked by perisciatic administration of antagonists of IL-6, TNF and IL-1, supporting the conclusion that multiple inflammatory mediators, acting at the level of the inflamed sciatic nerve, are involved in the creation of SIN-induced pain enhancement [28]. In addition, Milligan et al. [17] have shown that mirror-image pain in the SIN model was prevented or reversed by intrathecal pro-inflammatory cytokine antagonists specific for interleukin-1, tumor necrosis factor, or interleukin-6. Reversal of mirror-image pain was rapid and complete even when SIN was maintained constantly for 2 weeks before proinflammatory cytokine antagonist administration. These results, plus the results obtained in the present study with IL-1αβ (−/−) mice provide further evidence that ipsilateral and mirror-image neuropathic pain are created both acutely and chronically through glial and pro-inflammatory cytokine actions.

Previous research has shown that IL-1 release can alter many pronociceptive mechanisms including NMDA, NO, COX-2, SP and NGF [30] and that the pronociceptive actions of IL-1 may be more pronounced under conditions of tonic neurotransmitter release such as ongoing inflammation [16,25]. Thus, the antinociceptive phenotype exhibited by IL-1αβ (−/−) mice in chronic pain models may reflect a diversity of actions of IL-1 in both inflammatory and nerve injury pain states. The present data provide the first detailed characterization of the nociceptive phenotype of mice lacking genes for both IL-1 isoforms in models of chronic inflammatory and neuropathic pain. In these models of chronic nociception, IL-1αβ (−/−) mice show significantly attenuated nociceptive sensitivity compared to control mice and the magnitude of this difference is generally greater than that found for acute pain models [31]. Previous studies of genetic knockout mice involving different aspects of IL-1β signaling have noted the potential for compensatory developmental changes within the IL-1 system as a source of ambiguity in mechanistic interpretations of the resulting phenotype [3,27]. Indeed, developmental compensation is a general concern in genetic knockout experiments [9]. However, the present characterization of mice lacking both isoforms of IL-1 eliminates a potential confound regarding potential developmental alterations of IL-1α. Since IL-1αβ (−/−) mice were capable of generating inflammation-evoked TNFα to the same degree as BALB/c controls, genetic disruption of both IL-1α and IL-1β does not appear to produce broad changes in cytokine function [12]. In this regard, the expression of the IL-1ra and TNFα has been reported to be unaltered in IL-1 gene disrupted mice [12]. Additionally, the apparent unaltered ability of IL-1αβ (−/−) mice to generate TNFα, may provide some insight into the resulting nociceptive phenotype of IL-1αβ (−/−) mice. Analysis of the pronociceptive cytokine cascade underlying carrageenan-induced inflammation has provided evidence for both TNF-specific and IL-1-dependent nociceptive pathways [6]. Ferreira and colleagues [6] have recently demonstrated that TNFR-1 (−/−) mice show significantly less carraggeenan and keratinocyte-derived cytokine-induced hyperalgesia as compared to wild-type mice. Thus, inflammation-evoked increases in TNF likely contribute to the expression of nociception observed in chronic pain models.

In conclusion, the present results confirm the role of IL-1 in acute pain states and extend the role of this pro-inflammatory cytokine in chronic pain states. These data demonstrate that IL-1αβ modulates both the generation and the maintenance of inflammatory and chronic neuropathic pain and that IL-1 may modulate nociceptive sensitivity to a greater extent in conditions of chronic as compared to acute pain. In addition, these results suggest that in the chronic constriction injury model of neuropathic pain, IL-1 plays a role in the development and maintenance of mirror-image pain.

References

[1] Bennett GJ, Xie YK. A peripheral mononeuropathy in rat that produces disorders of pain sensation like those seen in man. Pain 1988;33:87–107.

[2] Bianchi M, Dib B, Panerai AE. Interleukin-1 and nociception in the rat. J Neurosci Res 1998;53:645–50.

[3] Boutin H, LeFeuvre RA, Horai R, Asano M, Iwakura Y, Rothwell NJ. Role of IL-1α and IL-1β in ischemic brain damage. J Neurosci 2001;21:5528–34.

[4] Brennan TJ, Vandermeulen EP, Gebhart GF. Characterization of a rat model of incisional pain. Pain 1996;64(3):493–501.

[5] Chaplan SR, Bach FW, Pogrel JW, Chung JM, Yaksh TL. Quantitative assessment of tactile allodynia in the rat paw. J Neurosci Meth 1994;53:55–63.

[6] Cunha TM, Verri WA, Silva JS, Poole S, Cunha FQ, Ferreira AH. A cascade of cytokines mediates mechanical inflammatory hypernociception in mice. Proc Natl Acad Sci 2005;102:1755–60.

[7] Dinarello CA. Interleukin-1, interleukin-1 receptors and interleukin-1 receptor antagonist. Int Rev Immunol 1998;16:457–99.

[8] Ferreira S, Lorenzetti B, Bristow A, Poole S. Interleukin-1β as a potent hyperalgesic agent antagonized by a tripeptide analogue. Nature 1988;334:698–700.

[9] Gingrich JA, Hen R. The broken mouse: the role of development, plasticity and environment in the interpretation of phenotypic changes in knockout mice. Curr Opin Neurobiol 2000;10:146–52.

[10] Haley JE, Sullivan AF, Dickenson AH. Evidence for spinal *N*-methyl-D-aspartate receptor involvement in prolonged chemical nociception in the rat. Brain Res 1990;518:218–26.

[11] Hargreaves K, Dubner R, Brown F, Flores C, Joris J. A new and sensitive method for measuring thermal nociception in cutaneous hyperalgesia. Pain 1988;32:77–88.

[12] Horai R, Asano M, Sudo K, Kanuka H, Suzuki M, Nishihara M, et al. Production of mice deficient in genes for interleukin (IL)-1α, IL-1β, IL-1αβ, and IL-1 receptor antagonist shows that IL-1β is crucial in turpentine-induced fever development and glucocorticoid secretion. J Exp Med 1998;187:1463–75.

[13] Horai R, Saijo S, Tanioka H, et al. Development of chronic inflammatory arthropathy resembling rheumatoid arthritis in interleukin 1 receptor antagonist-deficient mice. J Exp Med 2000;191:313–20.

[14] Kim SH, Chung JM. An experimental model for peripheral neuropathy produced by segmental spinal nerve ligation in the rat. Pain 1992;50:355–63.

[15] Kowaluk EA, Wismer C, Mikusa J, Zhu C, Schweitzer E, Lynch JJ, et al. ABT-702, a novel orally effective adenosine kinase (AK) inhibitor analgesic with anti-inflammatory properties. II. Antinociceptive and anti-inflammatory effects in rat models of persistent, inflammatory, and neuropathic pain. J Pharmacol Exp Ther 2000;295:1165–74.

[16] Maier SF, Wietelak EP, Martin D, Watkins LR. Interleukin-1 mediates the behavioral hyperalgesia produced by lithium chloride and endotoxin. Brain Res 1993;623:321–4.

[17] Milligan ED, Twining C, Chacur M, Biedenkapp J, O'Connor K, Poole S, et al. Spinal glia and proinflammatory cytokines mediate mirror-image neuropathic pain in rats. J Neurosci 2003;23(3):1026–40.

[18] Nakae S, Asano M, Horai R, Iwakura Y. Interleukin-1β, but not interleukin 1α, is required for T-cell-dependent antibody production. Immunology 2001;104:402–9.

[19] Oguri S, Motegi K, Iwakura Y, Endo Y. Primary role of interleukin-1α and interleukin-1β in lipopolysaccharide-induced hypoglycemia in mice. Clin Diag Lab Immunol 2002;9:1307–12.

[20] Perretti M, Solito E, Parente L. Evidence that endogenous interleukin-1 is involved in leukocyte migration in acute experimental inflammation in rats and mice. Agents Actions 1992;35(1–2):71–8.

[21] Pogatzki EM, Raja-Srinivasa. A mouse model of incisional pain. Anesthesiology 2003;99:1023–7.

[22] Safieh-Garabedian B, Poole S, Allchorne A, Winter J, Woolf CJ. Contribution of interleukin-1 to the inflammation-induced increase in nerve growth factor levels and inhlammatory hyperalgesia. Br J Pharmacol 1995;115:1265–75.

[23] Schreiber K, Beitz A, Wilcox G. Chronic contralateral pain in a unilateral carrageenan mouse model: role of spinal cord inflammatory mediators. Am Pain Soc 2003:821B.

[24] Sommer C, Petrausch S, Lindenlaub T, Toyka KV. Neutralizing antibodies to interleukin1-receptor reduce pain-associated behavior in mice with experimental neuropathy. Neurosci Lett 1999;270: 25–8.

[25] Tadano T, Namioka M, Nakagawasai O, Tan-No K, Matsushima K, Endo Y, et al. Induction of nociceptive responses by intrathecal injection of interleukin-1 in mice. Life Sci 1999;65:255–61.

[26] Torok K, Nemeth K, Erdo F, Aranyi P, Szekely JI. Measurement and drug induced modulation of interleukin-1 level during zymosan peritonitis in mice. Inflamm Res 1995;44(6):248–52.

[27] Touzani O, Boutin H, LeFeurve R, Parker L, Miller A, Luheshi G, et al. Interleukin-1 influences ischemic brain damage in the mouse independently of the interleukin-1 type 1 receptor. J Neurosci 2002;22:38–43.

[28] Twining C, Sloane EM, Milligan ED, Chacur M, Martin D, Poole S, et al. Peri-sciatic proinflammatory cytokines, reactive oxygen species, and complement induce mirror-image neuropathic pain in rats. Pain 2004;110:299–309.

[29] Watkins LR, Wiertelak EP, Goehler LE, Smith KP, Martin D, Maier SF. Characterization of cytokine-induced hyperalgesia. Brain Res 1994;654:15–26.

[30] Wiertelak EP, Furness LE, Watkins LR, Maier SF. Illness-induced hyperalgesia is mediated by a spinal NMDA-nitric oxide cascade. Brain Res 1994;664:9–16.

[31] Wolf G, Yirmiya R, Goshen I, Iverfeldt K, Holmlund L, Takeda K, et al. Impairment of interleukin-1 (IL-1) signaling reduces basal pain sensitivity in mice: genetic, pharmacological and developmental aspects. Pain 2004;104:471–80.

[32] Zahn PK, Brennan TJ. Intrathecal metabotropic glutamate receptor antagonists do not decrease mechanical hyperalgesia in a rat model of postoperative pain. Anesth Analg 1998;87(6):1354–9.

Journal of Neuroscience Research 83:119–133 (2006)

Disease Progression of Human SOD1 (G93A) Transgenic ALS Model Rats

Arifumi Matsumoto,[1,3,6] Yohei Okada,[1,4,6] Masanori Nakamichi,[5] Masaya Nakamura,[2] Yoshiaki Toyama,[2] Gen Sobue,[4] Makiko Nagai,[3] Masashi Aoki,[3] Yasuto Itoyama,[3] and Hideyuki Okano[1,6]★

[1]Department of Physiology, Keio University School of Medicine, Tokyo, Japan
[2]Department of Orthopaedic Surgery, Keio University School of Medicine, Tokyo, Japan
[3]Department of Neurology, Tohoku University Graduate School of Medicine, Sendai, Japan
[4]Department of Neurology, Nagoya University Graduate School of Medicine, Nagoya, Japan
[5]Takeda Chemical Industries, Ltd., Osaka, Japan
[6]Core Research for Evolutional Science and Technology (CREST), Japan Science and Technology Agency (JST), Saitama, Japan

The recent development of a rat model of amyotrophic lateral sclerosis (ALS) in which the rats harbor a mutated human SOD1 (G93A) gene has greatly expanded the range of potential experiments, because the rats' large size permits biochemical analyses and therapeutic trials, such as the intrathecal injection of new drugs and stem cell transplantation. The precise nature of this disease model remains unclear. We described three disease phenotypes: the forelimb-, hindlimb-, and general-types. We also established a simple, non-invasive, and objective evaluation system using the body weight, inclined plane test, cage activity, automated motion analysis system (SCANET), and righting reflex. Moreover, we created a novel scale, the Motor score, which can be used with any phenotype and does not require special apparatuses. With these methods, we uniformly and quantitatively assessed the onset, progression, and disease duration, and clearly presented the variable clinical course of this model; disease progression after the onset was more aggressive in the forelimb-type than in the hindlimb-type. More importantly, the disease stages defined by our evaluation system correlated well with the loss of spinal motor neurons. In particular, the onset of muscle weakness coincided with the loss of approximately 50% of spinal motor neurons. This study should provide a valuable tool for future experiments to test potential ALS therapies.

Key words: amyotrophic lateral sclerosis; evaluation system; behavioral analyses; phenotype; variability

Amyotrophic lateral sclerosis (ALS) is a fatal neurodegenerative disorder that mainly affects the upper and lower motor neurons (de Belleroche et al., 1995). It is characterized by progressive muscle weakness, amyotrophy, and death from respiratory paralysis, usually within 3–5 years of onset (Brown 1995). Although most cases of ALS are sporadic (SALS), approximately 10% are familial (FALS) (Mulder et al., 1986). Moreover, 20–25% of FALS cases are due to mutations in the gene encoding copper-zinc superoxide dismutase (SOD1) (Deng et al., 1993; Rosen et al., 1993). More than 100 different mutations in the SOD1 gene have been identified in FALS so far.

Until recently, animal models of FALS have been various transgenic mice that express a mutant human SOD1 (hSOD1) gene. Of these, a transgenic mouse carrying the G93A (Gly-93 → Ala) mutant hSOD1 gene was the first described (Gurney et al., 1994) and is used all over the world because this model closely recapitulates the clinical and histopathological features of the human disease. To evaluate the therapeutic effects of potential ALS treatments in this animal, many motor-related behavioral tasks are used (Chiu et al., 1995; Barneoud et al., 1997; Garbuzova-Davis et al., 2002; Sun et al., 2002; Wang et al., 2002; Inoue et al., 2003; Kaspar et al., 2003; Weydt et al., 2003; Azzouz et al., 2004). However, transgenic mice have innate limitations for some types of experiments because of their small size.

Recently, transgenic rat models of ALS, which harbor the hSOD1 gene containing the H46R (His-46 → Arg) or G93A mutation were generated (Nagai et al., 2001). The larger size of these rat models makes certain experiments easier, such as biochemical analyses that require large amounts of sample, intrathecal administration

Contract grant sponsor: Core Research for Evolutional Science and Technology (CREST), Japan Science and Technology Agency (JST); Contract grant sponsor: Japanese Ministry of Health, Labour and Welfare; Contract grant sponsor: Japanese Ministry of Education, Culture, Sports, Science and Technology.

*Correspondence to: Hideyuki Okano, Department of Physiology, School of Medicine, Keio University, 35 Shinanomachi, Shinjuku-ku, Tokyo, 160-8582, Japan. E-mail: hidokano@sc.itc.keio.ac.jp

Received 22 August 2005; Revised 29 September 2005; Accepted 30 September 2005

Published online 7 December 2005 in Wiley InterScience (www.interscience.wiley.com). DOI: 10.1002/jnr.20708

of drugs, and, especially, therapeutic trials, including the transplantation of neural stem cells into the spinal cord. The hSOD1 (G93A) transgenic rats typically present weakness in one hindlimb first. Later, weakness progresses to the other hindlimb and to the forelimbs. Finally, the rats usually become unable to eat or drink, and eventually die. Only subjective and ambiguous analyses were made with regard to the clinical progression of this ALS animal model and objective criteria for evaluating the efficacy of these new treatments have not been determined. For these reasons, we assessed the disease progression quantitatively using five different measures (body weight, inclined plane test, cage activity, SCANET, and righting reflex) and established an easy, noninvasive, and objective evaluation system that is sensitive to small but important abnormalities in the hSOD1 (G93A) transgenic rats. In addition, we created a novel scale, the Motor score, to assess disease progression in the transgenic rats without using special apparatuses. We also examined the validity of these measures as assessment tools for the pathology by investigating the number of spinal motor neurons remaining at the disease stages defined by each measure.

MATERIALS AND METHODS

Transgenic Rats

All animal experiments were conducted according to the Guidelines for the Care and Use of Laboratory Animals of Keio University School of Medicine. We used hSOD1 (G93A) transgenic male rats (Nagai et al., 2001) from our colony and their age- and gender-matched wild-type littermates as controls. Rats were housed in a specific pathogen-free animal facility at a room temperature of 23 ± 1°C under a 12-hr light-dark cycle (light on at 08:00). Food (solid feed CE-2, 30kGy; CLEA Japan, Inc.) and water were available ad lib. Transgenic rats were bred and maintained as hemizygotes by mating transgenic males with wild-type females. Transgenic progeny were identified by detecting the exogenous hSOD1 transgene, by amplification of pup tail DNA extracted at 20 days of age by polymerase chain reaction (PCR). The primers and cycling conditions were described previously (Nagai et al., 2001).

Exploration of Assessment Tools to Measure Disease Progression in the hSOD1 (G93A) Transgenic Rats

We evaluated the usefulness of four different measures to assess disease progression in the transgenic rats. All tests were carried out between 12:00–16:00 and in a double-blind fashion.

Body weight. Animals ($n = 9$ for each genotype) were weighed weekly after 30 days of age with an electronic scale. To avoid overlooking the beginning of weight loss, the animals were weighed every second or third day after 90 days of age, the age at which motor neurons are reported to be lost in the lumbar spinal cord (Nagai et al., 2001).

Inclined plane. This test was initially established mainly to assess the total strength of the forelimbs and hindlimbs in a model of spinal cord injury (Rivlin and Tator, 1977). Briefly, rats were placed laterally against the long axis of the inclined plane, and the maximum angle at which they could maintain their position on the plane for 5 sec was measured. To assess the strength of both sides of limbs equally, animals were placed on the inclined plane with the right side of the body to the downhill side of the incline, and then with the left side of the body facing downhill. For each rat, the test was carried out three times for each side, and the mean value of the angles obtained for the right side was compared to that obtained for the left. The lower mean value was recorded as the angle for that rat. Animals ($n = 9$ for each genotype) were tested weekly after 70 days of age and every second to third day after 100 days of age.

Cage activity. Animals ($n = 8$ for each genotype) were housed individually and monitored every day for all 24 hr (except for the days the cages were changed) after they were 70 days old. Spontaneous locomotor activity in the home cage (345 × 403 × 177 mm) was recorded by an activity-monitoring system (NS-AS01; Neuroscience, Inc., Tokyo, Japan) as described previously (Ohki-Hamazaki et al., 1999). The sensor detects the movement of animals using the released infrared radiation associated with their body temperature. The data were analyzed by the DAS-008 software (Neuroscience, Inc., Tokyo, Japan). To eliminate data variability owing to differences in the baseline movement of each rat, the baseline value was calculated as the mean of movement from 70–90 days of age, during which all rats were considered to move normally. We analyzed the data at each time point as the percentage of the baseline value in defining disease onset with this test.

SCANET. For short-term activity, 10 min of spontaneous activity was measured with the automated motion analysis system SCANET MV-10 (Toyo Sangyo Co., Ltd., Toyama, Japan) (Mikami et al., 2002). Animals ($n = 4$ for each genotype) were tested weekly after 30 days of age and every second or third day after 100 days of age. Each rat was individually placed in the SCANET cage for 10 min. Three parameters were measured: small horizontal movements of 12 mm or more (Move 1; M1), large horizontal movements of 60 mm or more (Move 2; M2), and the frequency of vertical movements caused by rearing (RG). To distinguish RG movements from incomplete standing actions, the upper sensor frame was adjusted to 13 cm above the lower sensor frame.

Righting reflex. All affected animals were tested for the ability to right themselves within 30 sec of being turned on either side (righting reflex) (Gale et al., 1985). Failure was seen when animals reached the end-stage of disease (Howland et al., 2002), and was regarded as a generalized loss of motor activity. We used this time point, which we call "end-stage," as "death" rather than the actual death of the animal, to exclude the influence of poor food intake and respiratory muscle paralysis on the survival period. All end-stage animals were sacrificed after being deeply anesthetized.

All statistical analyses were carried out with the two-tailed unpaired Student's t-test. A P-value of <0.05 was considered statistically significant.

Motor Score

To establish our own scoring system for motor function, which could be uniformly applicable to any disease phenotype of this rat model, we examined the common clinical findings

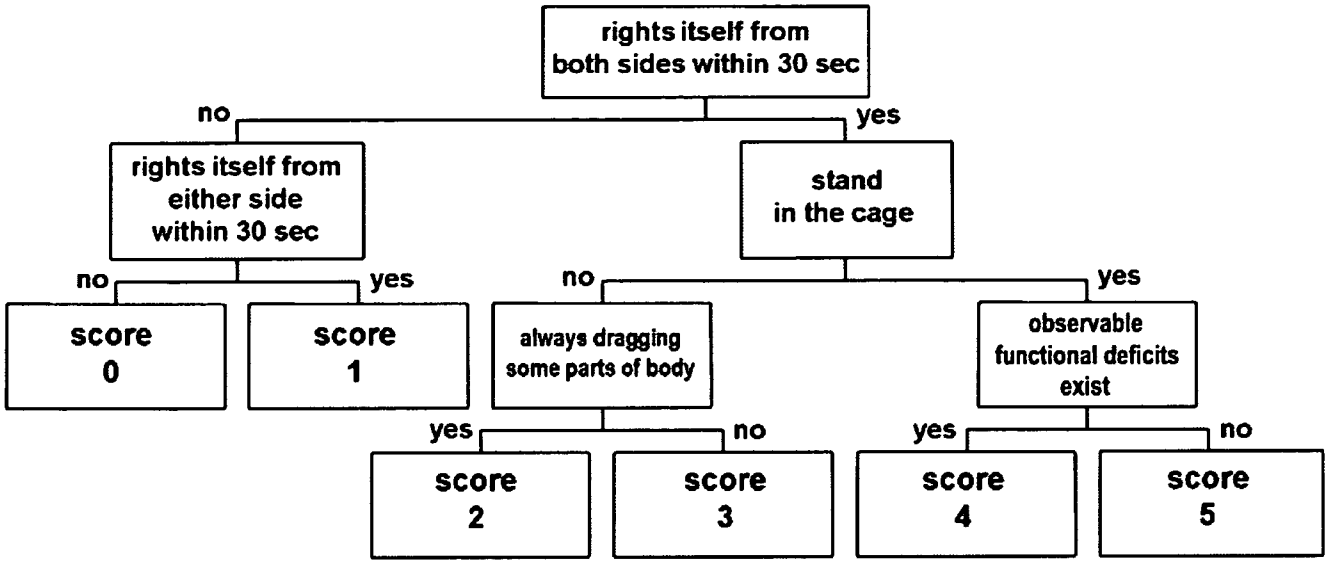

Fig. 1. Chart of Motor score assessment. The degree of motor dysfunction can be assessed by the Motor score as shown in this chart. This scoring system is meant to be used after disease onset, which can be prospectively diagnosed by the inclined plane test (muscle weakness onset). A score of 4 means the same condition as seen for subjective onset (SO). Rats with a score of 5 seem almost as normal as wild-type rats. The detailed testing procedure for the Motor score is described in the text.

of the transgenic rats in detail and assessed their motor functions ($n = 20$). We focused on the following tests: the righting reflex, the ability to stand in the cage, the extent of dragging their bodies when moving, and the existence of observable functional deficits. We evaluated these items sequentially along with the disease progression and classified the rats into six groups by giving them scores between 0 and 5. The scoring chart (Motor score) is shown in Figure 1.

When disease onset in the rats was diagnosed by their scoring $<70°$ on the inclined plane test (muscle weakness onset), the affected rats were tested for righting reflex. If they were unable to right themselves from either side, they were given a score of 0. If they could right themselves from only one side but not the other, they were given a score of 1.

Rats that could right themselves from both sides were examined for the ability to stand in the cage as follows: Rats were observed in the home cage for 1 min to see if they would stand spontaneously (Step 1). When they moved little in the home cage or showed no tendency to stand during Step 1, they were stimulated by being transferred to another cage (Step 2), and then by being returned to their home cage again (Step 3); the transfers were done to activate exploration motivation. During Step 3, the rats were further stimulated by lightly knocking the cage to intensify the motivation to explore. Each step was carried out for 1 min and the test was stopped when the rat stood once. Rats were judged as "unable to stand" if they did not stand, even after all three steps.

Rats that did not stand were subjected to the next test in the open field, where the extent to which they dragged their bodies when moving was assessed. Those who always dragged and could not lift some parts of their bodies except for scrotums and tails at any time were given a score of 2. If they could lift their dragging parts off the ground for even a moment, they were given a score of 3. The phenotype of dragging the forelimbs was different from that of dragging the hindlimbs. As disease progressed, "forelimb-type" rats first began to touch the tips of their noses on the ground, and then began to drag their head and upper trunk as they moved backward with their hindlimbs. "Hindlimb-type" rats dragged their lower trunk and moved forward with their forelimbs.

Finally, rats that had no abnormality in the above-mentioned assessments were examined in detail to see whether they had any observable functional deficits such as paralysis of the limbs or symptoms of general muscle weakness (e.g., walking with a limp, sluggish movement) in the open field. This condition could be judged subjectively and was defined as subjective onset. Rats with any of these symptoms were given a score of 4; otherwise they were given a score of 5.

Because the scores were based on subjective judgment, they might vary depending on the examiner. To examine inter-rater variability, three transgenic rats of different clinical types were examined according to the method described above, recorded on video tape, and subsequently scored by five observers from different backgrounds (Table I). The scores classified by the five observers were statistically analyzed for inter-rater agreement using Cohen's κ statistics (Table II). Kappa values can range from 0 (no agreement) to 1.00 (perfect agreement), and can be interpreted as poor (<0.00), slight (0.00–0.20), fair (0.21–0.40), moderate (0.41–0.60), substantial (0.61–0.80), and almost perfect (0.81–1.00) (Landis and Koch, 1977). The scores for the three transgenic rats were, on the whole, quite consistent among the five observers, suggesting that the Motor score can be used as an objective method for assessing disease progression.

TABLE I. Motor Score of Transgenic Rats Assessed by Five Different Observers

Transgenic rat	Observer	Days after onset (days) 0	1	2	3	4	5	6	7	8
#1407 Eventual hindlimb type										
	A	5	4	4		2	2	1	0	
	B	4	4	4		2	2	1	0	
	C	4	4	4		2	2	1	0	
	D	4	4	4		2	2	1	0	
	E	4	4	4		2	2	1	0	
	Mean	4.2	4	4		2	2	1	0	
#1470 Pure hindlimb type										
	A	5		4	4	2	2	2	2	0
	B	5		4	3	3	2	2	2	0
	C	5		4	3	2	2	2	2	0
	D	4		4	4	2	2	2	2	0
	E	4		4	3	2	2	2	2	0
	Mean	4.6		4	3.4	2.2	2	2	2	0
#1449 Pure forelimb type										
	A	4	3	3	3		2	1	1	0
	B	4	3	3	3		2	1	1	0
	C	3	3	3	3		2	1	1	0
	D	3	3	3	3		2	1	1	0
	E	4	3	2	2		2	1	1	0
	Mean	3.6	3	2.8	2.8		2	1	1	0

TABLE II. The kappa Statistics for Inter-Rater Agreement of Motor Score

Observers	Transgenic rat (clinical type) #1407 Eventual hindlimb	#1470 Pure hindlimb	#1449 Pure forelimb
A vs. B	0.82	0.69	1.00
A vs. C	0.82	0.82	0.83
A vs. D	0.82	0.81	0.83
A vs. E	0.82	0.70	0.69
B vs. C	1.00	0.83	0.83
B vs. D	1.00	0.53	0.83
B vs. E	1.00	0.66	0.69
C vs. D	1.00	0.64	1.00
C vs. E	1.00	0.82	0.54
D vs. E	1.00	0.81	0.54

TABLE III. Clinical Types of hSOD1 (G93A) Transgenic Rats

Clinical type	Subtype	*n*	%
Forelimb	Pure	4	8.2
	Eventual	5	10.2
Hindlimb	Pure	19	38.7
	Eventual	17	34.7
General		4	8.2
Total		49	100

Real-Time RT-PCR and Western Blot Analysis

Tissue specimens were dissected from the cerebral cortices, cerebella, medullae, and spinal cords (cervical, thoracic, and lumbar spinal cords) of the deeply anesthetized rats, and divided into two portions for total RNA and total protein preparation. Total RNA was isolated and first strand cDNA was synthesized as described previously (Okada et al., 2004). The real time RT-PCR analysis was carried out using Mx3000P (Stratagene, La Jolla, CA) with SYBR Premix Ex Taq (Takara Bio, Inc., Otsu, Japan). The primers used for the analysis were human *SOD1* (5′-TTGGGCAATGTGACTGCTGAC-3′, 5′-AGCTAGCAGGATAACAGATGA-3′), rat *SOD1* (5′-ACTTCGAGCAGAAGGCAAGC-3′, 5′-ACATTGGCCACACCGTCCTTTC-3′), and *β-actin* (5′-CGTGGGCCGCCCTAGGCACCA-3′, 5′-TTGGCCTTAGGGTTCAGAGGGG-3′). The results are presented as ratios of mRNA expression normalized to an inner control gene, *β-actin*. Total protein was prepared in lysis buffer containing 10 mM Tris-HCl (pH 7.6), 50 mM NaCl, 30 mM sodium pyrophosphate, 50 mM sodium fluoride, 20 mM glycerophosphate, 1% Triton X-100, and a protease inhibitor mixture (Complete; Roche Applied Science, Mannheim, Germany). Western blot analysis was carried out by a method established previously. In brief, a 5 μg protein sample of an extract was run on 12% SDS-PAGE, transferred to nitrocellulose, and probed with anti-human SOD1 (1:1,000, mouse IgG, Novocastra Laboratories, Ltd., Benton Lane, UK), and anti-α-tubulin (1:2,000, mouse IgG, Sigma-Aldrich, Inc., Saint Louis, MO). Signals were detected with HRP-conjugated secondary antibodies (Jackson ImmunoResearch Laboratories, Inc., West Grove, PA) using an ECL kit (Amersham Bioscience UK limited, Little Chalfont, UK). Quantitative analysis was carried out with a Scion Image (Scion Corporation, Frederick, MD). The amounts of proteins loaded in each slot were normalized to those of α-tubulin.

Immunohistochemical Analysis

Rats were deeply anesthetized (ketamine 75 mg/kg, xylazine 10 mg/kg, i.p.) and transcardially perfused with 4% paraformaldehyde/PBS (0.1 M PBS, pH 7.4) for histological examination. Spinal cord tissues were dissected out and post-fixed overnight in the same solution. Each spinal cord was dissected into segments that included the C6, T5, and L3 levels, immersed in 15% sucrose/PBS followed by 30% sucrose/PBS at 4°C, and embedded in Tissue-Tek O.C.T. Compound (Sakura Finetechnical Co., Ltd., Tokyo, Japan). Embedded tissue was immediately frozen with liquid nitrogen and stored at −80°C. Serial transverse sections of each spinal segment were cut on a cryostat at a thickness of 14 μm. The sections were pre-treated with acetone for 5 min, rinsed with PBS three times and permeabilized with TBST (Tris-buffered saline with 1% Tween 20) for 15 min at room temperature. After being blocked in the TNB buffer (Perkin-Elmer Life Sciences, Inc., Boston, MA) for 1 hr at room temperature, the sections were incubated at 4°C overnight with an anti-choline acetyltransferase (ChAT) polyclonal antibody (AB144P, Goat IgG, 1:50; Chemicon International, Inc., Temecula, CA). After being washed with PBS three times, the sections were incubated for 2 hr at room temperature with a biotinylated secondary antibody (Jackson ImmunoResearch Laboratories, Inc.). Finally, the labeling was developed using the avidin-biotin-peroxidase complex procedure (Vectastain ABC kits; Vector Laboratories, Inc., Burlingame, CA) with 3,3-diaminobenzidine (DAB; Wako Pure Chemical Industries, Ltd., Osaka, Japan) as the chro-

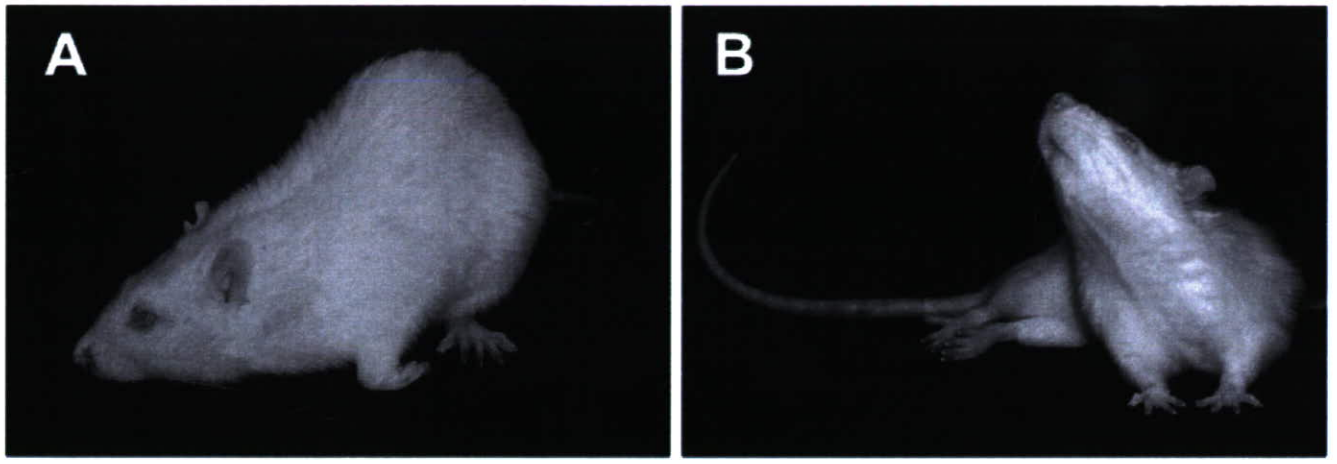

Fig. 2. Characteristic appearance of hSOD1 (G93A) transgenic rats. **A:** Forelimb type. The rat was unable to raise its head and was obligated to take a posture of raising the lumbar region, as indicated, because of the paralyzed forelimbs. **B:** Hindlimb type. The rat showed paraplegia, but was able to raise its head and upper trunk with its non-paralyzed forelimbs.

mogen. Immunohistochemical images were examined with a Zeiss-AxioCam microscope system.

Motor neurons bearing ChAT-immunoreactivity in laminae VII, VIII, and IX of the ventral horn were counted in every tenth section (5 sections total for each segment) for each of the C6, T5, and L3 segments. Only the neurons that showed labeling above background level and were larger than 20 μm in diameter were counted. The numbers of motor neurons in all segments (C6, T5, and L3) were summed for each animal to evaluate not only the local motor neuron loss, but the generalized loss of motor neurons throughout the spinal cord of each animal ($n = 3$ for each genotype at each time point). We next examined the correlation between the number of residual motor neurons and the results of the functional analyses described in this study. Statistical analysis was carried out with two-tailed unpaired Student's *t*-test. A *P*-value of <0.05 was considered statistically significant.

RESULTS

Clinical Types of hSOD1 (G93A) Transgenic Rats

Because we noticed variations in the disease phenotypes expressed by the G93A rats, we classified 49 rats into three clinical categories according to the location of initial paralysis. The clinical types were: the forelimb type, hindlimb type, and general type (Table III). Rats whose paralysis started in the forelimbs and progressed to the hindlimbs were defined as the "forelimb type." In contrast, rats whose paralysis started from the hindlimbs and progressed to the forelimbs were defined as the "hindlimb type." A typical appearance for the forelimb and hindlimb types is shown in Figure 2. Other rats, which showed simultaneous paralysis in the forelimbs and hindlimbs, were categorized as the "general type".

In addition, we classified the forelimb- and hindlimb-type rats into two subtypes, the pure and eventual types, based on the timing of the initial paralysis (Table III). Rats of the pure type showed paralysis that was limited to one or more of the four limbs as the initial observable deficit. Those of the eventual type initially showed symptoms of general muscle weakness (e.g., walking with a limp, sluggish movement), but without unequivocal limb paralysis. In the eventual type animals, paralysis of one of the limbs became apparent later. The ratio of each subtype is shown in Table III.

Evaluation of Disease Progression in the hSOD1 (G93A) Transgenic Rats

Although the transgenic rats varied in their clinical types, all four measures of disease progression (body weight, inclined plane test, cage activity, and SCANET) showed significant differences between the transgenic and wild-type rats (Fig. 3).

In contrast to the continuous weight gain in wild-type rats, the body weight in the affected rats ceased to increase and gradually decreased, with peak body weight attained around 110–120 days of age ($P < 0.05$, after 112 days of age) (Fig. 3A).

In the inclined plane test, initially both the transgenic and wild-type rats uniformly scored 75–80 degrees, after several training trials. However, the transgenic rats showed a significant decline in performance compared to their wild-type littermates from 120 days of age (Fig. 3B).

In the cage activity measurement, the movements of the wild-type rats remained stable, whereas those of the transgenic rats declined rapidly after 125 days of age (Fig. 3C).

In the SCANET test, even the wild-type rats showed decreased movements for all parameters (M1, M2, RG) in the late observation period, though they showed no abnormality in their motor functions. This might be because they had acclimated to the SCANET cage. The movement score of the transgenic rats was consistently worse than that of the wild-type rats after

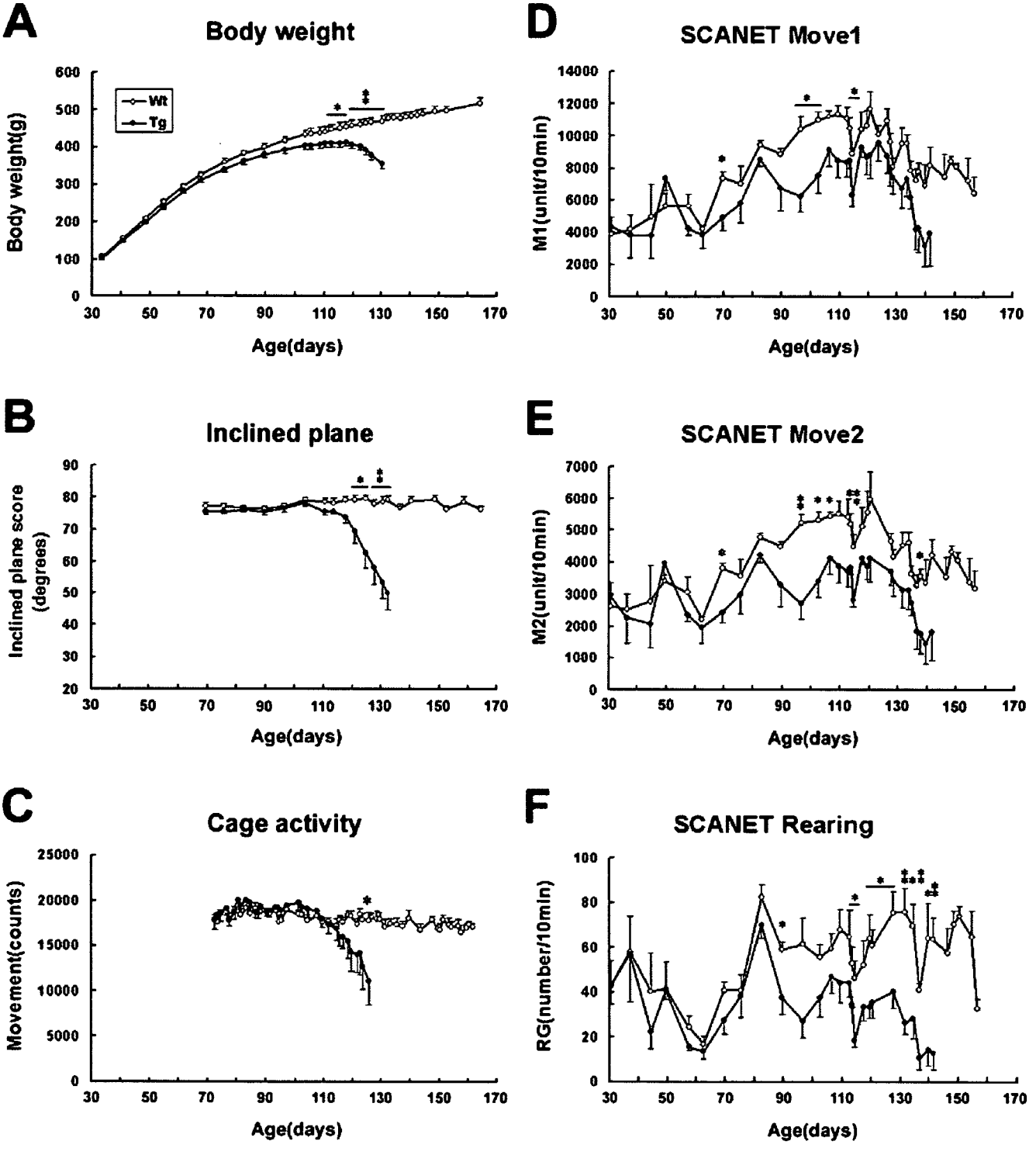

Fig. 3. Disease progression in hSOD1 (G93A) transgenic rats monitored by four effective measures. **A:** Body weight. The weight gain of the transgenic group stopped at around 110–120 days. The difference became statistically significant at 112 days of age ($n = 9$ for each genotype). **B:** Inclined plane. The wild-type group scored 75–80° throughout the period, whereas the score of the transgenic group declined. The difference became statistically significant at 120 days of age ($n = 9$ for each genotype). **C:** Cage activity. The movements of the wild-type group were stable, whereas the scores of the transgenic group declined. Significance was reached at 125 days of age ($n = 8$ for each genotype). **D–F:** SCANET. For all parameters (M1, M2, RG), the movement scores of the transgenic group became constantly worse than those of the wild-type group after 60 days of age. The differences between the groups increased markedly after 90 days of age. Significance was attained beginning at 67 days of age for M1 and M2, and at 87 days of age for RG ($n = 4$ for each genotype). The comparison between the wild-type and transgenic groups was stopped when the first of the transgenic rats reached the end-stage of the disease and was sacrificed. Mean ± SEM. $^{*}P < 0.05$. $^{**}P < 0.01$; two-tailed unpaired Student's t-test.

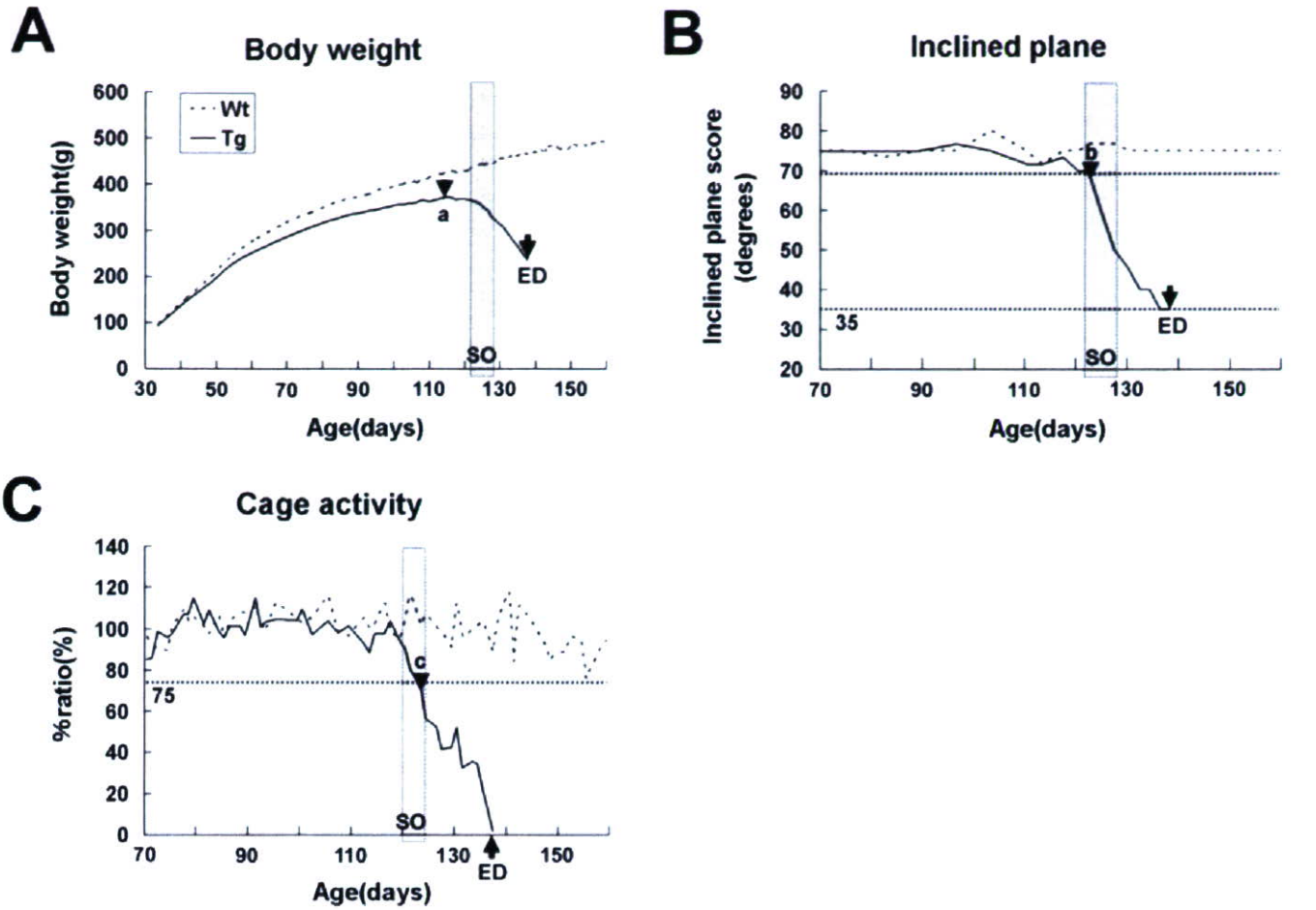

Fig. 4. Schematic presentation of the results from the body weight (**A**), inclined plane test (**B**), and cage activity (**C**) assessments. The onset defined by each measure (black arrowheads) and the end-stage of the disease (ED, black arrows) are indicated in the figures. a, pre-symptomatic onset: the day the transgenic rats scored their maximum body weight. b, muscle weakness onset: the earliest day the transgenic rats scored <70° in the inclined plane test. c, hypo-activity onset: the earliest day the transgenic rats scored <75% of the mean movements from 70–90 days of age in the cage activity measure. SO, subjective onset: the earliest day that observable functional deficits such as paralysis of the limbs or symptoms of general muscle weakness were observed subjectively in the open field (the gray shaded region in A–C).

60 days of age for all parameters (M1, M2, RG), however, even after the wild-type animals showed the decrease in their movement scores. The differences between the two groups increased markedly after 90 days of age for M1, M2, and RG (Fig. 3D–F). The performance of each rat fluctuated so markedly that the SCANET test seems to be inappropriate for statistical analysis.

Onset, End-Stage, and Duration of Disease in hSOD1 (G93A) Transgenic Rats

Using the quantitative analysis of disease progression by body-weight measurement, the inclined plane test, and cage activity, as described above, we defined three time points of "objective onset," as shown in Figure 4. The SCANET results did not allow us to define a time of objective onset, because we could not establish a stable baseline level using the data from the highly variable measurements we obtained, even for wild-type rats. The righting reflex failure was useful for detecting the time point of end-stage disease, which we defined as the generalized loss of motor activity in affected rats. A total of 20 transgenic rats assessed by body weight and the inclined plane test were analyzed for the day of objective onset, end-stage, and duration of the disease. The cage activity data from the eight transgenic rats were obtained simultaneously. The results are shown in Table IV.

The day the transgenic rats reached their maximum body weight was defined as pre-symptomatic onset (113.6 ± 4.8 days of age, black arrowhead in Fig. 4A, Table IV). This onset was judged retrospectively and always preceded the subjective onset (gray shaded region, Fig. 4A), which was determined by observable functional deficits in the open field, such as paralysis of limbs and symptoms of general muscle weakness. The